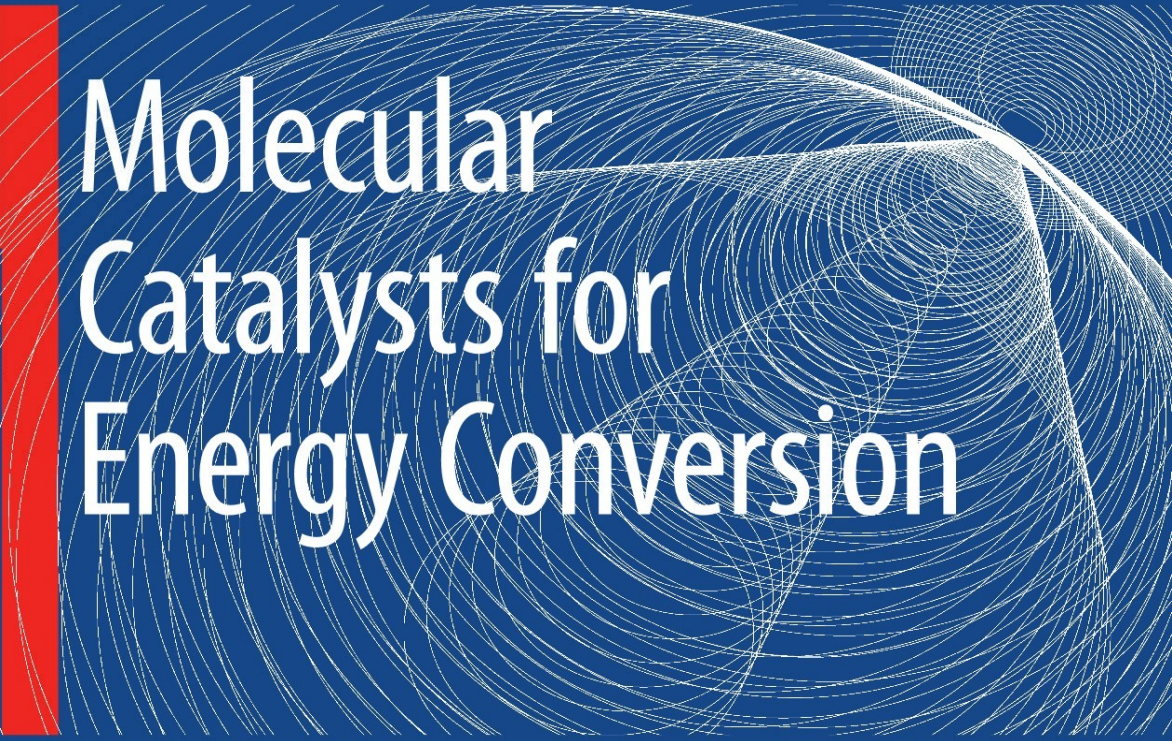


Tatsuhiro Okada  
Masao Kaneko  
*Editors*

SPRINGER SERIES IN MATERIALS SCIENCE 111



# Molecular Catalysts for Energy Conversion

 Springer



# Springer Series in MATERIALS SCIENCE

---

*Editors:* R. Hull   R. M. Osgood, Jr.   J. Parisi   H. Warlimont

The Springer Series in Materials Science covers the complete spectrum of materials physics, including fundamental principles, physical properties, materials theory and design. Recognizing the increasing importance of materials science in future device technologies, the book titles in this series reflect the state-of-the-art in understanding and controlling the structure and properties of all important classes of materials.

- |     |  |     |  |
|-----|--|-----|--|
| 99  | <b>Self-Organized Morphology<br/>in Nanostructured Materials</b><br>Editors: K. Al-Shamery and J. Parisi                                     | 109 | <b>Reactive Sputter Deposition</b><br>Editors: D. Depla and S. Mahieu  |
| 100 | <b>Self Healing Materials</b><br>An Alternative Approach<br>to 20 Centuries of Materials Science<br>Editor: S. van der Zwaag                 | 110 | <b>The Physics of Organic Superconductors<br/>and Conductors</b><br>Editor: A. Lebed   |
| 101 | <b>New Organic Nanostructures<br/>for Next Generation Devices</b><br>Editors: K. Al-Shamery, H.-G. Rubahn,<br>and H. Sitter                  | 111 | <b>Molecular Catalysts<br/>for Energy Conversion</b><br>Editors: T. Okada and M. Kaneko  |
| 102 | <b>Photonic Crystal Fibers</b><br>Properties and Applications<br>By F. Poli, A. Cucinotta,<br>and S. Selleri                                 | 112 | <b>Atomistic and Continuum Modeling<br/>of Nanocrystalline Materials</b><br>Deformation Mechanisms<br>and Scale Transition<br>By M. Cherkaoui and L. Capolungo |
| 103 | <b>Polarons in Advanced Materials</b><br>Editor: A.S. Alexandrov   | 113 | <b>Crystallography<br/>and the World of Symmetry</b><br>By S.K. Chatterjee   |
| 104 | <b>Transparent Conductive Zinc Oxide</b><br>Basics and Applications<br>in Thin Film Solar Cells<br>Editors: K. Ellmer, A. Klein, and B. Rech | 114 | <b>Piezoelectricity</b><br>Evolution and Future of a Technology<br>Editors: W. Heywang, K. Lubitz,<br>and W. Wersing   |
| 105 | <b>Dilute III-V Nitride Semiconductors<br/>and Material Systems</b><br>Physics and Technology<br>Editor: A. Erol                             | 115 | <b>Lithium Niobate</b><br>Defects, Photorefraction<br>and Ferroelectric Switching<br>By T. Volk and M. Wöhlecke  |
| 106 | <b>Into The Nano Era</b><br>Moore's Law Beyond Planar Silicon CMOS<br>Editor: H.R. Huff  | 116 | <b>Einstein Relation<br/>in Compound Semiconductors<br/>and Their Nanostructures</b><br>By K.P. Ghatak, S. Bhattacharya, and D. De                             |
| 107 | <b>Organic Semiconductors<br/>in Sensor Applications</b><br>Editors: D.A. Bernards, R.M. Ownes,<br>and G.G. Malliaras                        | 117 | <b>From Bulk to Nano</b><br>The Many Sides of Magnetism<br>By C.G. Stefanita   |
| 108 | <b>Evolution of Thin-Film Morphology</b><br>Modeling and Simulations<br>By M. Pelliccione and T.-M. Lu                                       |     |  |

---

Volumes 50–98 are listed at the end of the book.

Tatsuhiko Okada  
Masao Kaneko

Editors

# Molecular Catalysts for Energy Conversion

With 286 Figures

 Springer

Dr. Tatsuhiro Okada

National Institute of Advanced Industrial Science and Technology  
Higashi 1-1-1, Tsukuba, Ibaraki 305-8565, Japan  
E-mail: okada.t@aist.go.jp

Professor Dr. Masao Kaneko

The Institute of Biophotochemonics, Co. Ltd.  
Bunkyo 2-1-1, 310-8512 Mito, Ibaraki, Japan  
E-mail: mkaneko@mx.ibaraki.ac.jp

*Series Editors:*

Professor Robert Hull

University of Virginia  
Dept. of Materials Science and Engineering  
Thornton Hall  
Charlottesville, VA 22903-2442, USA

Professor Jürgen Parisi

Universität Oldenburg, Fachbereich Physik  
Abt. Energie- und Halbleiterforschung  
Carl-von-Ossietzky-Strasse 9-11  
26129 Oldenburg, Germany

Professor R. M. Osgood, Jr.

Microelectronics Science Laboratory  
Department of Electrical Engineering  
Columbia University  
Seeley W. Mudd Building  
New York, NY 10027, USA

Professor Hans Warlimont

Institut für Festkörper-  
und Werkstofforschung,  
Helmholtzstrasse 20  
01069 Dresden, Germany

Springer Series in Materials Science ISSN 0933-033X

ISBN 978-3-540-70730-1

e-ISBN 978-3-540-70758-5

Library of Congress Control Number: 2008931404

© Springer-Verlag Berlin Heidelberg 2009

This work is subject to copyright. All rights are reserved, whether the whole or part of the material is concerned, specifically the rights of translation, reprinting, reuse of illustrations, recitation, broadcasting, reproduction on microfilm or in any other way, and storage in data banks. Duplication of this publication or parts thereof is permitted only under the provisions of the German Copyright Law of September 9, 1965, in its current version, and permission for use must always be obtained from Springer-Verlag. Violations are liable to prosecution under the German Copyright Law.

The use of general descriptive names, registered names, trademarks, etc. in this publication does not imply, even in the absence of a specific statement, that such names are exempt from the relevant protective laws and regulations and therefore free for general use.

Typesetting: Data prepared by SPi using a Springer TeX macro package  
Cover concept: eStudio Calamar Steinen  
Cover production: WMX Design GmbH, Heidelberg

SPIN: 12024605 57/3180/SPi  
Printed on acid-free paper

9 8 7 6 5 4 3 2 1

springer.com

---

## Preface

Over the past decade the topic of energy and environment has been acknowledged among many people as a critical issue to be solved in 21st century since the Kyoto Protocol came into effect in 1997. Its political recognition was put forward especially at Heiligendamm in 2007, when the effect of carbon dioxide emission and its hazard in global climate were discussed and shared universally as common knowledge. Controlling the global warming in the economical framework of massive development worldwide through this new century is a very challenging problem not only among political, economical, or social circles but also among technological or scientific communities. As long as the humans depend on the combustion of fossil for energy resources, the waste heat exhaustion and CO<sub>2</sub> emission are inevitable.

In order to establish a new era of energy saving and environment benign society, which is supported by technologies and with social consensus, it is important to seek for a framework where new clean energy system is incorporated as infrastructure for industry and human activities. Such a society strongly needs innovative technologies of least CO<sub>2</sub> emission and efficient energy conversion and utilization from remaining fossil energies on the Earth. Energy recycling system utilizing natural renewable energies and their conversion to hydrogen may be the most desirable option of future clean energy society. Thus the society should strive to change its energy basis, from fossil-consuming energy to clean and recycling energy.

In the future “clean energy society,” a closed hydrogen cycle consisting of hydrogen generation, storage, transmission, and usage that are driven by a solar energy as the energy source is to be established. For such purpose, water photoelectrolysis, photosynthesis from CO<sub>2</sub> to bioenergy, electrochemical solar cells, and fuel cells should be the most important combinations of technologies. In this sense, a dream of humans toward sustainable energy society should be realized with hydrogen-mediated energy conversion systems.

Technological background for such dream is being enforced by a wide spectrum of researches in above-mentioned fields. Fuel cells and artificial photosynthesis are the most developing fields in the last few decades. One of the key

technologies for such developments should be the electrocatalysts for electrochemical energy conversion. The efficiency and utilization of energy conversion highly depend on the electrocatalysts that determine the reaction route, energy barrier through the rate-controlling process, and frequency factor. The history of electrocatalysts dates back to the beginning of 20th century, when electrode kinetics started to be investigated with the language of the “current and overpotential.” For an energy conversion system, Sir William R. Grove first proposed a model of fuel cell in 1839 using hydrogen and oxygen gases with platinum electrocatalysts. Today many researchers aim to invent and investigate new electrocatalysts for variety of electrochemical reactions, and such trend will continue to look for the most efficient and cost-competitive catalyst materials.

A new possibility of electrocatalysts is proposed in this context, which would assist in developing vast field of electrocatalysts. The organic complex catalysts for energy conversion, which are emerging technologies in the last several decades, are the main topic of the book focusing on energy and environment technologies. Such molecular catalysts have wide variety of applications in the field of fuel cell technology, electrochemical solar cells, artificial photosyntheses, and so on. Since these molecular catalysts have many potential advantages over inorganic or metal-alloy catalysts due to their cost performance, capability of manipulating structures through molecular design and synthesis, variety of immobilization processes on the catalyst substrate, etc., a firm strategy for their design and application is awaited to cope with the expeditious solution of the latest energy and environment issues.

This book aims to provide a scientific and technological basis for the design and application of molecular catalysts for energy conversion and environment protection, and to establish a method of efficient processing, manufacturing, and development. This book is expected to be beneficial for those people who are studying, researching, or developing molecular catalysts as the electrocatalysts or photocatalysts in energy conversion systems.

Chapter 1 introduces the historical overview and the underlying designing concepts of molecular catalysts with the scope of new developing field. Chapters 2 through 3 give fundamental aspects of the elementary reactions associated with the electrocatalytic processes and measuring techniques of molecular catalysts. From Chaps. 4 to 7, developing fields of molecular catalysts in fuel-cell energy conversion systems are discussed with variety of examples in the anode and the cathode of the reacting gas systems. Chapters 8 through 10 give another new field of molecular catalysts, and electrochemical solar cells and photosynthesis technology are presented with examples of dye-sensitizers for photochemical reactions, nano-materials for photoelectrodes and charge-transport media. Chapters 11 and 12 discuss new applications of molecular catalysts in environmental cleaning and in sensor technology. Chapters 13–15 provide fundamental knowledge for the catalyst researches, which are indispensable tools for understanding elementary molecular processes in the electrocatalytic and photocatalytic processes. Finally Chap. 16 gives the summary

and future prospects of molecular catalysts in the energy conversion technology in various possible fields of applications.

This book is contributed by many of the renowned authors in the related field of researches, and chapters are arranged through intent discussions and interplay of authors and editors. It is carefully planned so that all the chapters keep good balances and therefore provide the readers with adequate state-of-the-art technologies and knowledge concerning the newly emerging field of molecular catalysts for energy conversion. Lastly we would like to express our hearty acknowledgments to all the contributors and to the staff of Springer Verlag for their willing interest and generous assistance, without which this book would not have been published in success.

Tsukuba  
Mito  
July 2008

*Tatsuhiko Okada*  
*Masao Kaneko*



---

# Contents

<b>Preface</b> .....	V
<b>List of Contributors</b> .....	XVII
<b>List of Abbreviations</b> .....	XXI
<b>1 Historical Overview and Fundamental Aspects of Molecular Catalysts for Energy Conversion</b>	
<i>T. Okada, T. Abe, and M. Kaneko</i> .....	1
1.1 Introduction: Why Molecular Catalysts? A New Era of Biomimetic Approach Toward Efficient Energy Conversion Systems.....	1
1.2 Molecular Catalysts for Fuel Cell Reactions .....	2
1.2.1 Oxygen Reduction Catalysts .....	3
1.2.2 Fuel Oxidation Catalysts .....	13
1.3 Molecular Catalysts for Artificial Photosynthetic Reaction .....	17
1.3.1 Water Oxidation Catalyst .....	18
1.3.2 Reduction Catalyst .....	18
1.3.3 Photodevices for Photoinduced Chemical Reaction in the Water Phase .....	25
1.4 Summary .....	29
References .....	30
<b>2 Charge Transport in Molecular Catalysis in a Heterogeneous Phase</b>	
<i>M. Kaneko and T. Okada</i> .....	37
2.1 Introduction .....	37
2.2 Charge Transport (CT) by Molecules in a Heterogeneous Phase ..	38
2.2.1 General Overview .....	38
2.2.2 Mechanism of Charge Transport .....	39
2.3 Charge Transfer by Molecules Under Photoexcited State in a Heterogeneous Phase .....	46

2.3.1	Overview	46
2.3.2	Mechanism of Charge Transfer at Photoexcited State in a Heterogeneous Phase	47
2.4	Charge Transfer and Electrochemical Reactions in Metal Complexes	50
2.4.1	Charge Transfer in Metal Complexes	50
2.4.2	Charge Transfer at Electrode Surfaces	53
2.4.3	Oxygen Reduction Reaction at Metal Macrocycles	55
2.5	Proton Transport in Polymer Electrolytes	59
2.5.1	Proton Transfer Reactions	59
2.5.2	Proton Transport in Polymer Electrolytes	60
2.6	Summary	62
	References	63
<b>3 Electrochemical Methods for Catalyst Evaluation in Fuel Cells and Solar Cells</b>		
	<i>T. Okada and M. Kaneko</i>	67
3.1	Introduction	67
3.2	Electrochemical Measuring System for Catalyst Research in Fuel Cells	68
3.2.1	Reference Electrode	68
3.2.2	Rotating Ring-Disk Electrode	69
3.2.3	Gas Electrodes of Half-Cell Configuration	74
3.2.4	Fuel Cell Test Station	76
3.2.5	Electrochemical Methods for Electrocatalysts	79
3.3	Electrochemical Measuring System for Heterogeneous Charge Transport and Solar Cells	86
3.3.1	Testing Method of Charge Transport in Heterogeneous Systems	86
3.3.2	Evaluation of Charge Transport by Redox Molecules Incorporated in a Heterogeneous Phase	88
3.3.3	AC Impedance Spectroscopy to Evaluate Charge Transport, Conductivity, Double-Layer Capacitance, and Electrode Reaction	89
3.3.4	I-V Characteristics of Solar Cells	93
3.3.5	Impedance Spectroscopy to Evaluate Multistep Charge Transport of a Dye-Sensitized Solar Cell	94
3.4	Summary	97
	References	101
<b>4 Molecular Catalysts for Fuel Cell Anodes</b>		
	<i>T. Okada</i>	103
4.1	Introduction	103
4.2	Concept of Composite Electrocatalysts in Fuel Cells	105
4.3	Methanol Oxidation Reaction	107

4.3.1	Mechanism of Methanol Oxidation Reaction . . . . .	107
4.3.2	New Electrocatalysts for Methanol Oxidation Reaction . . . . .	108
4.3.3	Structure of Composite Catalysts . . . . .	112
4.4	Formic Acid Oxidation Reaction . . . . .	118
4.4.1	Mechanism of Formic Acid Oxidation . . . . .	118
4.4.2	Formic Acid Oxidation on Composite Catalysts . . . . .	119
4.5	CO-Tolerant Electrocatalysts for Hydrogen Oxidation Reaction . . . . .	123
4.5.1	Electrochemical and Fuel Cell Testing . . . . .	123
4.5.2	Durability Testing . . . . .	127
4.5.3	Structural Characterization . . . . .	129
4.6	Summary . . . . .	134
	References . . . . .	135
<b>5 Macrocycles for Fuel Cell Cathodes</b>		
	<i>K. Oyaizu, H. Murata, and M. Yuasa</i> . . . . .	139
5.1	Introduction . . . . .	139
5.2	Molecular Design of Macrocycles for Fuel Cell Cathodes . . . . .	141
5.3	Diporphyrin Cobalt Complexes and Related Catalysts . . . . .	142
5.3.1	Diporphyrin Cobalt Complexes . . . . .	142
5.3.2	Polypyrrole Cobalt Complexes . . . . .	144
5.3.3	Cobalt Thienylporphyrins . . . . .	149
5.4	Porphyrin Assemblies Based on Intermolecular Interaction . . . . .	153
5.5	Multinuclear Complexes as Electron Reservoirs . . . . .	158
5.6	Summary . . . . .	159
	References . . . . .	160
<b>6 Platinum-Free Catalysts for Fuel Cell Cathode</b>		
	<i>N. Koshino and H. Higashimura</i> . . . . .	163
6.1	Introduction . . . . .	163
6.2	Drawbacks of Using Pt as Catalysts in PEFC . . . . .	164
6.3	Mechanistic Aspects of Oxygen Reduction by Cathode Catalyst . . . . .	165
6.4	Platinum-Free Catalysts for Fuel Cell Cathode . . . . .	166
6.4.1	Metal Particles . . . . .	167
6.4.2	Metal Oxides, Carbides, Nitrides, and Chalcogenides . . . . .	168
6.4.3	Carbon Materials . . . . .	171
6.4.4	Metal Complex-Based Catalysts . . . . .	172
6.4.5	Catalysts Designed from Dinuclear Metal Complexes . . . . .	177
6.5	Summary . . . . .	180
	References . . . . .	181
<b>7 Novel Support Materials for Fuel Cell Catalysts</b>		
	<i>J. Nakamura</i> . . . . .	185
7.1	Introduction . . . . .	185
7.2	Performance of Electrocatalysts Using Carbon Nanotubes . . . . .	187
7.2.1	H <sub>2</sub> -O <sub>2</sub> Fuel Cell . . . . .	187

7.2.2	DMFC	191
7.3	Why Is Carbon Nanotube So Effective as Support Material?	194
	References	197

## 8 Molecular Catalysts for Electrochemical Solar Cells and Artificial Photosynthesis

	<i>M. Kaneko</i>	199
8.1	Introduction	199
8.2	Overview on Principles of Molecule-Based Solar Cells	200
8.2.1	Photon Absorption	201
8.2.2	Suppression of Charge Recombination to Achieve Effective Charge Separation	201
8.2.3	Diffusion of Separated Charges	202
8.2.4	Electrode Reaction	202
8.3	Dye-Sensitized Solar Cell (DSSC)	202
8.4	Artificial Photosynthesis	208
8.5	Dark Catalysis for Artificial Photosynthesis	211
8.5.1	Dark Catalysis for Water Oxidation	212
8.5.2	Dark Catalysis for Proton Reduction	213
8.6	Conclusion and Future Scopes	213
	References	214

## 9 Molecular Design of Sensitizers for Dye-Sensitized Solar Cells

	<i>K. Hara</i>	217
9.1	Introduction	217
9.2	Metal-Complex Sensitizers	219
9.2.1	Molecular Structures of Ru-Complex Sensitizers	219
9.2.2	Electron-Transfer Processes	224
9.2.3	Performance of DSSCs Based on Ru Complexes	226
9.2.4	Other Metal-Complex Sensitizers for DSSCs	229
9.3	Porphyrins and Phthalocyanines	230
9.4	Organic Dyes	231
9.4.1	Molecular Structures of Organic-Dye Sensitizers for DSSCs	231
9.4.2	Performance of DSSCs Based on Organic Dyes	236
9.4.3	Electron Transfer from Organic Dyes to TiO <sub>2</sub>	237
9.4.4	Electron Diffusion Length	240
9.5	Stability	242
9.5.1	Photochemical and Thermal Stability of Sensitizers	242
9.5.2	Long-Term Stability of Solar-Cell Performance	243
9.6	Summary and Perspectives	244
	References	245

## 10 Fabrication of Charge Carrier Paths for High Efficiency Cells

<i>T. Kogo, Y. Ogomi, and S. Hayase</i> .....	251
10.1 Introduction .....	251
10.2 Fabrication of Electron-Paths .....	252
10.3 Suppression of Black-Dye Aggregation in a Pressurized CO <sub>2</sub> Atmosphere .....	255
10.4 Two-Layer TiO <sub>2</sub> Structure for Efficient Light Harvesting .....	256
10.5 TCO-Less All-Metal Electrode-Type DSC .....	257
10.6 Ion-Path in Quasi-Solid Medium .....	257
10.7 Summary.....	260
References .....	260

## 11 Environmental Cleaning by Molecular Photocatalysts

<i>D. Wöhrle, M. Kaneko, K. Nagai, O. Suworova, and R. Gerdes</i> .....	263
11.1 Introduction .....	263
11.2 Oxidative Methods for the Photodegradation of Pollutants in Wastewater.....	264
11.2.1 Comparison of Different Methods of UV Processes for Water Cleaning .....	264
11.2.2 Photodegradation of Pollutants with Oxygen in the Visible Region of Light .....	268
11.3 Visible Light Decomposition of Ammonia to Nitrogen with Ru(bpy) <sub>3</sub> <sup>2+</sup> as Sensitizer.....	287
11.3.1 Nitrogen Pollutants and Their Photodecomposition .....	287
11.3.2 Photochemical Electron Relay with Ammonia .....	287
11.3.3 Photochemical Decomposition of Ammonia to Dinitrogen by a Photosensitized Electron Relay .....	290
11.4 Visible Light Responsive Organic Semiconductors as Photocatalysts.....	291
11.4.1 Photoelectrochemical Character of Organic Semiconductors in Water Phase .....	291
11.4.2 Photoelectrochemical Oxidations by Irradiation with Visible Light .....	292
11.4.3 Photochemical Decomposition of Amines Using Visible Light and Organic Semiconductors .....	293
References .....	294

## 12 Optical Oxygen Sensor

<i>N. Asakura and I. Okura</i> .....	299
12.1 Introduction .....	300
12.2 Theoretical Aspect of Optical Oxygen Sensor of Porphyrins .....	300
12.2.1 Advantage of Optical Oxygen Sensing.....	300
12.2.2 Principle of Optical Oxygen Sensor .....	301
12.2.3 Brief History of Optical Oxygen Sensors.....	303

12.3	Optical Oxygen Sensor by Phosphorescence Intensity .....	304
12.3.1	Phosphorescent Compounds .....	304
12.3.2	Immobilization of Phosphorescent Molecules for Optical Oxygen Sensor and Measurement System.....	304
12.3.3	Optical Oxygen Sensor with Platinum Octaethylporphyrin Polystyrene Film (PtOEP-PS Film) .....	307
12.3.4	Optical Oxygen Sensor with PtOEP and Supports.....	309
12.3.5	Application of Optical Oxygen Sensor for Air Pressure Measurements.....	311
12.4	Optical Oxygen Sensor by Phosphorescence Lifetime Measurements .....	313
12.4.1	Advantages of Phosphorescence Lifetime Measurement ...	313
12.4.2	Phosphorescence Lifetime Measurement .....	314
12.4.3	Distribution of Oxygen Concentration Inside Single Living Cell by Phosphorescence Lifetime Measurement .....	315
12.5	Optical Oxygen Sensor T-T Absorption .....	318
12.5.1	Advantage of Optical Oxygen Sensor Based on T-T Absorption .....	320
12.5.2	Optical Oxygen Sensor Based on the Photoexcited Triplet Lifetime Measurement .....	320
12.5.3	Optical Oxygen Sensor Based on Stationary T-T Absorption (Stationary Quenching) .....	325
12.6	Summary.....	327
	References .....	327
<b>13 Adsorption and Electrode Processes</b>		
	<i>H. Shiroishi</i> .....	329
13.1	Introduction .....	329
13.2	Adsorption Isotherms and Kinetics .....	330
13.2.1	Langmuir Isotherms .....	330
13.2.2	Freundlich Isotherm .....	332
13.2.3	Temkin Isotherm .....	332
13.2.4	Application for Selective Reaction on Metal Surface by Adsorbate.....	334
13.3	Slab Optical Waveguide Spectroscopy .....	339
13.3.1	Principle .....	340
13.3.2	Application of Slab Optical Waveguide Spectroscopy .....	342
13.4	Methods of Digital Simulation for Electrochemical Measurements .....	344
13.4.1	Formulation of Electrochemical System .....	344
13.4.2	Finite Differential Methods .....	351
13.5	Digital Simulation for Polymer-Coated Electrodes .....	354
13.5.1	Hydrostatic Condition .....	355
13.5.2	Hydrodynamic Condition.....	357

13.6 Classical Monte Carlo Simulation for Charge Propagation in Redox Polymer .....	358
13.6.1 Visualization of Charge Propagation .....	359
13.6.2 Determination of a Charge Hopping Distance .....	361
References .....	363
<b>14 Spectroscopic Studies of Molecular Processes on Electrocatalysts</b>	
<i>A. Kuzume and M. Ito</i> .....	367
14.1 Introduction .....	367
14.2 The Preparation and Spectroscopic Characterization of Fuel Cell Catalysts .....	369
14.2.1 Catalyst Preparation by Electroless Plating and Direct Hydrogen Reduction Methods: Practical Application for High Performance PEFC .....	369
14.2.2 In Situ IRAS Studies of Methanol Oxidation on Fuel Cell Catalysts .....	377
14.3 Spectroscopic Studies of Methanol Oxidation on Pt Surfaces .....	382
14.3.1 Electrooxidation of Methanol on Pt(111) in Acid Solutions: Effects of Electrolyte Anions during Electrocatalytic Reactions .....	382
14.3.2 Methanol Oxidation Mechanisms on Pt(111) Surfaces .....	388
14.4 Conclusions .....	392
References .....	393
<b>15 Strategies for Structural and Energy Calculation of Molecular Catalysts</b>	
<i>S. Tsuzuki and M. Saito</i> .....	395
15.1 Introduction .....	395
15.2 Computational Methods .....	396
15.3 Basis Set and Electron Correlation Effects on Geometry and Conformational Energy .....	397
15.4 Intermolecular Forces .....	397
15.5 Basis and Electron Correlation Effects on Intermolecular Interactions .....	398
15.6 Calculations of Transition Metal Complexes .....	402
15.7 Examples of the Ab Initio Calculation for Molecular Catalysts ...	402
15.8 Summary .....	409
References .....	409
<b>16 Future Technologies on Molecular Catalysts</b>	
<i>T. Okada and M. Kaneko</i> .....	411
16.1 Introduction .....	411
16.2 Road Map for Clean Energy Society .....	412
16.3 Hydrogen Production .....	415
16.3.1 Natural Gas .....	415

16.3.2 Renewable Energy Source .....	415
16.3.3 Biomass.....	417
16.4 Hydrogen Utilization.....	418
16.4.1 Hydrogen Storage .....	419
16.4.2 Energy Conversion .....	419
16.5 Biomimetic Approach and Role of Molecular Catalysts for Energy-Efficient Utilization .....	420
16.6 Summary.....	421
References .....	422
<b>Index .....</b>	<b>423</b>



---

## List of Contributors

### **Toshiyuki Abe**

Department of Frontier  
Materials Chemistry  
Graduate School of Science  
and Technology  
Hirosaki University  
3 Bunkyo-cho, Hirosaki 036-8561  
Japan  
tabe@cc.hirosaki-u.ac.jp

### **Noriyuki Asakura**

Department of Bioengineering  
Tokyo Institute of Technology  
Nagatsuta-cho, 4259, Midori-ku  
Yokohama 226-8501, Japan  
nasakura@bio.titech.ac.jp

### **Robert Gerdes**

Universität Bremen  
Institute of Organic and  
Macromolecular Chemistry  
P.O. Box 330440, 28334 Bremen  
Germany  
robert.gerdes@chemie.uni-bremen.de

### **Kohjiro Hara**

National Institute of Advanced  
Industrial Science and Technology  
Research Center for Photovoltaics  
1-1-1 Higashi, Tsukuba  
Ibaraki 305-8565, Japan  
k-hara@aist.go.jp

### **Shuji Hayase**

Graduate School of Life Science  
and Systems Engineering  
Kyushu Institute of Technology  
2-4 Hibikino, Wakamatsu-ku  
Kitakyushu 808-0196, Japan  
hayase@life.kyutech.ac.jp

### **Hideyuki Higashimura**

Tsukuba Laboratory  
Sumitomo Chemical Co., Ltd.  
6 Kitahara, Tsukuba  
Ibaraki 300-3294, Japan  
higashimura@sc.sumitomo-chem.co.jp

### **Masatoki Ito**

Department of Chemistry  
Faculty of Science and Technology  
Keio University  
Kohoku-ku, Yokohama 223-8522  
Japan  
masatoki@chem.keio.ac.jp

### **Masao Kaneko**

The Institute of Biophotochemonics  
Co. Ltd.  
2-1-1 Bunkyo, Mito 310-8512  
Japan  
mkaneko@mx.ibaraki.ac.jp

**Takeshi Kogo**

Graduate School of Life Science  
and Systems Engineering  
Kyushu Institute of Technology  
2-4 Hibikino, Wakamatsu-ku  
Kitakyushu 808-0196, Japan  
kogo-takeshi@edu.life.kyutech.ac.jp

**Nobuyoshi Koshino**

Tsukuba Laboratory  
Sumitomo Chemical Co., Ltd.  
6 Kitahara Tsukuba  
Ibaraki 300-3294, Japan  
koshinon@sc.sumitomo-chem.co.jp

**Akiyoshi Kuzume**

Department of Chemistry  
Faculty of Science and Technology  
Keio University, Kohoku-ku  
Yokohama 223-8522, Japan  
kuzume@chem.keio.ac.jp

**Hidenori Murata**

Department of Pure and Applied  
Chemistry  
Faculty of Science and Technology  
Tokyo University of Science  
Noda 278-8510, Japan  
himurata@rs.noda.tus.ac.jp

**Keiji Nagai**

Institute of Laser Engineering  
Osaka University  
2-6 Yamada-oka  
Suita Osaka 565-0871  
Japan  
knagai@ile.osaka-u.ac.jp

**Junji Nakamura**

Graduate School of Pure and Applied  
Sciences  
University of Tsukuba  
Tennoudai 1-1-1  
Tsukuba, Ibaraki 305-8573  
Japan  
nakamura@ims.tsukuba.ac.jp

**Yuhei Ogomi**

Graduate School of Life Science  
and Systems Engineering  
Kyushu Institute of Technology  
2-4 Hibikino  
Wakamatsu-ku  
Kitakyushu 808-0196, Japan  
ogomi-yuhei@edu.life.kyutech.ac.jp

**Tatsuhiko Okada**

Energy Technology Research  
Institute  
National Institute of Advanced  
Industrial Science and Technology  
Higashi 1-1-1, Tsukuba  
Ibaraki 305-8565, Japan  
okada.t@aist.go.jp

**Ichiro Okura**

Department of Bioengineering  
Tokyo Institute of Technology  
Nagatsuta-cho, 4259, Midori-ku  
Yokohama 226-8501, Japan  
iokura@bio.titech.ac.jp

**Kenichi Oyaizu**

Institute of Colloid and Interface  
Science  
Tokyo University of Science  
Noda 278-8510, Japan  
and Present Address:  
Department of Applied Chemistry  
Waseda University  
Tokyo 169-8555, Japan  
oyaizu@waseda.jp

**Morihiro Saito**

Department of Industrial  
Chemistry  
Faculty of Engineering  
Tokyo University of Science  
12-1 Ichigayafunagawara-machi  
Shinjuku-ku  
Tokyo 162-0826, Japan  
saitou.m@ci.kagu.tus.ac.jp

**Hidenobu Shiroishi**

Tokyo National College  
of Technology  
Kunugida 1220-2, Hachioji city  
Tokyo 193-0997, Japan  
h-shiroishi@tokyo-ct.ac.jp

**Olga Suvorova**

Russian Academy of Sciences  
Institute of Organometallic  
Chemistry  
GSP-445, Tropinina str. 49  
603950 Nizhnii Novgorod  
Russia

**Seiji Tsuzuki**

Research Institute of Computational  
Sciences  
National Institute of Advanced  
Industrial Science and Technology  
(AIST)  
1-1-1 Umezono, Tsukuba  
Ibaraki 305-8568, Japan  
s.tsuzuki@aist.go.jp

**Dieter Wöhrle**

Universität Bremen  
Institute of Organic  
and Macromolecular Chemistry  
P.O. Box 330440, 28334 Bremen  
Germany  
woehrle@chemie.uni-bremen.de

**Makoto Yuasa**

Department of Pure and Applied  
Chemistry  
Faculty of Science and Technology  
Tokyo University of Science  
and  
Institute of Colloid and Interface  
Science  
Tokyo University of Science  
Noda 278-8510  
Japan  
yuasa@rs.noda.tus.ac.jp

---

## List of Abbreviations

ADP	Adenosine-diphosphate (Sect. 2.5.1)
AFM	Atomic force microscopy (Sect. 1.2.2.1)
AM 1.5 G	Air mass 1.5 global-tilt (Sect. 9.1)
AOP	Advanced oxidation process (Sect. 11.2.1)
APCE	Absorbed photon-to-current conversion efficiency (Sect. 9.2.3)
ATP	Adenosine-triphosphate (Sect. 1.1, Sect. 2.5.1)
ATR	Attenuated total reflection (Sect. 9.2.1)
ATR-FTIR	Attenuated total reflectance Fourier transform infra-red spectroscopy (Sect. 4.4.1)
BET	Brunauer-Emmett-Teller (Sect. 5.3.2, Sect. 7.2.2)
BOD	Biological oxygen demand (Sect. 11.3.1)
BPCC	Biophotochemical cell (Sect. 8.4)
BSSE	Basis set superposition error (Sect. 15.2)
CB	Carbon black (Sect. 7.1, Sect. 14.1)
CCD	Coupled devise (Sect. 12.3.5)
CcO	Cytochrome <i>c</i> oxidase (Sect.5.1)
CCSD(T)	Coupled-cluster calculations with single and double substitutions with inclusion of noniterative triple excitations (Sect. 15.5)
CNT	Carbon nanotube (Sect. 7.1)
COD	Chemical oxygen demand (Sect. 11.3.1)
CT	Charge transport (Sect. 2.1)
CV	Cyclic voltammetry (Sect. 3.2.5, Sect. 14.1)
CW	Continuous wave (Sect. 12.5.3)
DFT	Density Functional Theory (Sect. 1.2.1.1, Sect. 13.2.4, Sect. 15.3)
DHE	Dynamic hydrogen electrode (Sect. 3.2.1)
DMFC	Direct methanol fuel cell (Sect. 1.2.2.2, Sect. 3.2.3, Sect. 4.3, Sect. 7.1, Sect. 13.1, Sect. 14.1)
DP	Proticity (proton motive force) (Sect. 2.5.1)

DSC	Dye-sensitized solar cell (Sect. 10.1)
DSSC	Dye-sensitized solar cell (Sect. 3.3.5, Sect. 8.1, Sect. 9.1)
DTA	Differential thermal analysis (Sect. 4.3.3)
EDX	Energy-dispersive X-ray analysis (Sect. 4.5.3)
EIS	Electrochemical impedance spectroscopy (Sect. 3.3.1)
EX	Explicit finite difference method (Sect. 13.4.2.2)
EXAFS	Extended X-ray absorption fine structure (Sect. 15.7, Sect. 4.3.3, Sect. 5.3.2)
FDM	Finite difference method (Sect. 13.4.2)
FE SEM	Field emission scanning electron microscope (Sect. 4.3.3)
FF	Fill factor (Sect. 3.3.4, Sect. 8.3)
FWHM	Full width half maximum (Sect. 14.3.1.2)
GDE	Gas diffusion electrodes (Sect. 7.2.1)
GDL	Gas diffusion layer (Sect. 3.2.4)
GGA	Generalized gradient approximation (Sect. 15.5)
HER	Hydrogen evolution reaction (Sect. 1.2.2.1)
HF	Hartree-Fock (Sect. 15.3)
HOMO	Highest occupied molecular orbital (Sect. 1.2.1.2, Sect. 5.3.2, Sect. 9.1, Sect. 15.7)
HOPG	Highly oriented pyrolytic graphite (Sect. 7.3)
HOR	Hydrogen oxidation reaction (Sect. 1.2.2.1, Sect. 15.7)
HREELS	High-resolution electron energy loss spectroscopy ( Sect. 14.3.2.1)
IEC	Ion exchange capacity (Sect. 2.5.2)
IMI	Intermittent microwave irradiation (Sect. 7.2.3)
IPCC	Intergovernmental Panel on Climate Change (Sect. 16.1)
IPCE	Incident photon-to-current conversion efficiency (Sect. 8.3, Sect. 9.2.3)
IR	Infrared spectroscopy (Sect. 14.1)
IRAS	Infrared reflection absorption spectroscopy (Sect. 14.1)
ISC	Intersystem crossing (Sect. 11.2.2)
ISO	International Standard Organization (Sect. 16.3.3)
ITO	Indium tin oxide (Sect. 2.2.2, Sect. 8.3, Sect. 13.2.2)
LCA	Lifecycle assessment (Sect. 16.3.3)
LEED	Low energy electron diffraction (Sect. 14.1)
LHE	Light-harvesting efficiency (Sect. 9.2.3)
LSD	Local spin density (Sect. 15.5)
LSV	Linear scanning voltammogram (Sect. 3.2.5)
LUMO	Lowest unoccupied molecular orbital (Sect. 9.1, Sect. 1.2.1.2, Sect. 15.7)
MB	Methylene blue (Sect. 11.2.2)
MEA	Membrane electrode assembly (Sect. 3.2.4, Sect. 5.1, Sect. 6.3, Sect. 7.1, Sect. 14.2.1)
MLCT	Metal-to-ligand charge transfer (Sect. 9.2.1)
MNc	Metal naphthalocyanines (Sect. 11.2.2)
MO	Molecular orbital (Sect. 2.4.3)

MOR	Methanol oxidation reaction (Sect. 4.3, Sect. 15.7)
MP	Metal porphyrin (Sect. 11.2.2)
MP2	Second-order Møller-Plesset perturbation calculations (Sect. 15.3)
MPc	Metal phthalocyanine (Sect. 11.2.2)
MV2+	Methylviologen (Sect. 2.2.2)
MWCNT	Multi-walled carbon nanotubes (Sect. 7.2.1)
Nd-YAG	Neodymium-Yttrium-Aluminum-Garnet (Sect. 12.4.3)
NE	Net energy (Sect. 16.3.2)
Nf	Nafion (Sect. 2.2.2)
NHE	Normal hydrogen electrode (Sect. 1.2.1, Sect. 3.2.1, Sect. 9.1, Sect. 11.2.1, Sect. 14.3.2.1)
NOW	Non-contact optical waveguide spectroscopy (Sect. 13.2.2)
ORR	Oxygen reduction reaction (Sect. 1.2.1, Sect. 2.4.3, Sect. 3.2.2, Sect. 6.1, Sect. 7.2.1, Sect. 15.7, Sect. 16.5)
OEC	Oxygen evolving center (Sect. 16.5)
PAH	Polycyclic aromatic hydrocarbons (Sect. 12.2.3)
PEFC	Polymer electrolyte fuel cell (Sect. 4.3, Sect. 6.1, Sect. 7.1, Sect. 14.1)
PEM	Polymer electrolyte membrane/proton-exchange membrane (Sect. 2.5.1)
PPy	Polypyrrole (Sect. 5.3.2)
PS	Photoelectron spectroscopy (Sect. 14.3.2.1)
PSCA	Potential-step chronoamperometry (Sect. 3.3.3)
PSCAS	Potential Step chronoamperometry (Sect. 2.2.2)
PTFE	Polytetrafluoroethylene (Sect. 14.2.1)
Q	Quencher (Sect. 2.3.2)
RB	Rose bengal (Sect. 11.2.2)
RDE	Rotating disk electrode (Sect. 3.2.2)
RHE	Reversible hydrogen electrode (Sect. 3.2.1, Sect. 4.4.2, Sect. 7.2.3)
RRDE	Rotating ring-disk electrode (Sect. 3.2.2)
SAED	Selected area electron diffraction (Sect. 14.2.1)
SCE	Saturated calomel electrode (Sect. 4.3.2, Sect. 5.3.2, Sect. 7.2.3, Sect. 9.2.1)
SCV	Spectroscopic voltammogram (Sect. 2.2.2)
SEIRAS	Surface enhanced infrared spectroscopy (Sect. 4.3.1, Sect. 13.3)
SEIRAS	Surface enhanced infrared reflection absorption spectroscopy (Sect. 14.3.2.2)
SHE	Standard hydrogen electrode (Sect. 3.2.1, Sect. 8.4)
SOWG	Slab optical waveguide (Sect. 13.1)
SPR	Surface plasmon resonance (Sect. 13.2.2)
STM	Scanning tunneling microscope (Sect. 1.2.2.1, Sect. 7.3)
TCO	Transparent conducting oxide (Sect. 9.1, Sect. 10.4)
TSC	Thermally stimulated current (Sect. 10.2)

XXIV List of Abbreviations

TEM	Transmission electron microscope (Sect. 4.3.3, Sect. 7.2.1, Sect. 14.1)
TG	Thermo-gravimetry (Sect. 4.3.3)
TOF-SIMS	Time-of-flight secondary ion mass spectroscopy (Sect. 6.4.4)
TPD	Temperature-programmed desorption (Sect. 7.3, Sect. 14.3.2.1)
T-T	Triplet-triplet (Sect. 12.5)
UHV	Ultra-high vacuum (Sect. 14.1)
UNEP	United Nations Environment Programme (Sect. 16.1)
UPD	Underpotential deposition (Sect. 4.4.1)
UV/Vis	Ultraviolet/visible (Sect. 13.3.1)
VUV	Vacuum ultraviolet process (Sect. 11.2.1)
WC	Tungsten carbide (Sect. 1.2.2.1, Sect. 6.4.2)
XANES	X-ray absorption near-edge structure (Sect. 4.3.3, Sect. 5.3.2)
XAS	X-ray absorption spectroscopy (Sect. 15.7)
XPS	X-ray photoelectron spectroscopy (Sect. 4.3.3, Sect. 7.3, Sect. 15.7)
XRD	X-ray diffraction (Sect. 4.3.3, Sect. 5.3.2, Sect. 6.4.2)

# Historical Overview and Fundamental Aspects of Molecular Catalysts for Energy Conversion

T. Okada, T. Abe, and M. Kaneko

**Abstract** In this chapter we focus on the historical background of the electrocatalysts especially of molecular catalysts that are considered as key technology for energy conversion systems. The energy conversion is a basic process with which humans can utilize natural energy by converting into useful forms of energy such as heat, electricity, or other secondary energies. The most important process to be established in this century will be the usage of renewable energy, which has least impact on the global environment. The central technologies for this process will be solar cells, photosynthesis, and fuel cells. Hydrogen energy society would be the most probable choice interconnecting these technologies, and toward this goal the establishment of efficient catalysts is indispensable. The designing of molecular catalysts is an important issue for solving the energy conversion yields and efficiency. Through biomimetic approaches many good candidates of catalysts for energy conversion have been studied. Porphyrins from cytochrome analogs have been studied since late 1960s as oxygen reduction center or oxygen carrier with variety of modifications. Also reduction of  $H^+$  is part of an artificial photosynthesis, and many supra-molecular and hybrid complexes are studied since 1970s. The chapter starts with the history and design concepts of oxygen reduction catalysts and fuel oxidation catalysts in fuel cells, to cope with the control of multi-electron transfer reactions. The state-of-the-art molecular catalysts are characterized as metal–nitrogen ligand complex or metal–nitrogen–oxygen conjugates on carbon support. Photochemical reduction of  $H^+$  is reviewed which is coupled to water oxidation, where historically metallophthalocyanines or polypyridyl complexes are studied intensively since mid-1980s. Charge separation antenna chlorophylls are models of dye-sensitizers for photoreductive  $H_2$  evolution, and these are incorporated in Graetzel cell for electrochemical solar cells. Design and application of molecular catalysts for these cells are reviewed.

## 1.1 Introduction: Why Molecular Catalysts? A New Era of Biomimetic Approach Toward Efficient Energy Conversion Systems

The principle of fuel cell was discovered as early as in 1839 by Sir William Grove [1]. He demonstrated the  $H_2$ – $O_2$  fuel cell with Pt electrodes contacting  $H_2$  and  $O_2$  gas reservoirs separated by  $H_2SO_4$  aqueous solution, which was



the first event that humans acquired electric energy generation with a feed of fuels. It is interesting to note that in the same year A. E. Becquerel discovered the principle of photoelectric effect when illuminating one of a pair of silver/silver halide electrodes in dilute acid [2]. Although Sir Grove's discovery was a big historical milestone, the technology needed 120 years further to find its major application when Gemini space flights implemented the mission with fuel cell power sources in 1960s. Also solar cells using silicon p-n junction were first established just in the mid-1950s. These facts symbolically show that the technology relies much on the development of material science for its true commercialization. For energy conversion systems, the efficiency seriously counts before they become of use.

The life on the earth flourished after the plant cells acquired the inherent energy conversion systems of solar energy 2,700 million years ago. Photosynthesis occurs in chloroplast of plant cells, and photon energy is converted to phosphorylation of  $H^+$ -ATPase and production of carbohydrate with more than 30% yield [3]. How the plants acquired such a high conversion efficiency is a very intriguing topic, but this leads us to an encouraging strategy that we mimic such sophisticated organs so that we finally obtain a system of high energy conversion using biomimetic materials.

After the Stone Age, the humans first invented tools for their lives mostly from minerals especially from metals. Alchemists in the medieval era extracted metal elements and synthesized materials from minerals. Today inorganic chemists and metallurgists use materials made from variety of elements in the periodic table. Although the number of inorganic materials is enormous, the community of organic chemists produces much more organic compounds almost unlimitedly. In the future of an advanced stage of biomimetic chemistry, humans will be able to synthesize such natural products as they like. It is therefore expected that we can achieve a high efficiency of energy conversion by adapting materials with biological concepts. This chapter intends to give an idea of how we produce new and useful catalysts for energy conversion in various fields, e.g., fuel cells, artificial photosynthesis, etc.

## 1.2 Molecular Catalysts for Fuel Cell Reactions

Fuel cells that operate at temperatures lower than  $100^\circ\text{C}$  and  $100\text{--}500^\circ\text{C}$  are categorized as "low-temperature fuel cells" and "medium-temperature fuel cells," respectively, and these include alkaline fuel cells, phosphoric acid fuel cells, polymer electrolyte fuel cells, and direct liquid-feed fuel cells [4, 5]. The common feature is that designing high performance electrocatalysts is crucial in order to achieve high-energy conversion in the gas (or liquid fuel) reactions that are occurring on an electron conducting solid phase.

Most of the elements on periodic table were surveyed as electrocatalyst as early as 1950s and for metal alloys by 1960s [4, 6]. The applications of these

elements were for chloralkali electrolysis, water electrolysis,  $\text{H}_2\text{O}_2$  production, and fuel cells. Investigations on fuel cell catalysts reached a commercial level when Davytan invented Ni- and Ag-supported active carbon electrodes for KOH alkaline fuel cells in 1950s. Sintered porous Ni electrodes by Bacon (1952) and Doppelskelett-Katalysator (DSK) electrodes made of Raney Ni or Pd by Justi (1954) were applied for alkaline fuel cells [4, 7]. Especially fuel cell catalysts were highlighted by many electrochemists during 1960s when NASA launched space mission projects. A big problem was “the sluggish character of  $\text{O}_2$  reduction,” as pointed out by U. R. Evans [8]. This limitation is due to the low reactivity of  $\text{O}_2$  that has electronically triplet ground state.

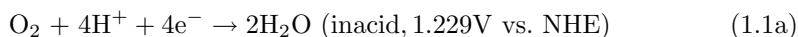
Slow kinetics require high-efficiency electrocatalysts. Materials usable for fuel cell catalysts are located near the center of the periodic table (around VIII<sub>a</sub> group metals), and especially those usable in acid media are only Pt or Pt-based alloys [4], which are less available than other components of fuel cells. It is inferred then if we rely on merely metal or alloy catalysts, we have very few possibilities to find innovative materials.

Organic metal complexes such as porphyrins and phthalocyanines attracted much attention as alternatives to precious metal catalysts since 1960s [9–11]. These are the basic components in hemes of oxygen transport or cytochrome C of respiratory chains [3, 12]. The peripheral ligand structures of pyrrole-N rings give the metal center an important function to adsorb  $\text{O}_2$  and transfer electrons to reduce it to  $\text{H}_2\text{O}$ . These molecules have a wide variety of molecular designing, and would be a potential candidate to tailor efficient electrocatalysts for fuel cell electrodes.

Historically nonmetallic catalysts have been studied for  $\text{O}_2$  reduction for almost 40 years, but recently some fuel oxidation catalysts for  $\text{H}_2$ ,  $\text{CH}_3\text{OH}$ , and  $\text{HCOOH}$  oxidation are also attracting interests as reported in the literature [13–15]. The fuel oxidation catalysts made from organic metal complexes are rather rare because Pt is the most active and practical material used in commercialized fuel cells since the NASA space era. Major concepts for designing organic metal complexes are to facilitate adsorption and dehydrogenation reactions of fuel molecules on the catalyst surface, and secondly to increase the tolerance against a by-product CO. In the following, fuel cell catalysts for oxygen reduction reaction and fuel oxidation reaction are reviewed and their designing strategy are discussed for structure optimization of organic metal complexes, based on postulated reaction mechanisms.

### 1.2.1 Oxygen Reduction Catalysts

The scheme for oxygen reduction reaction (ORR) in acid medium is depicted in Fig. 1.1 [16, 17]. The main process is four-electron reduction of  $\text{O}_2$  together with  $4\text{H}^+$ :



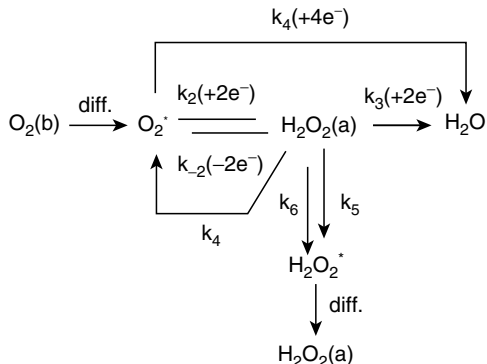
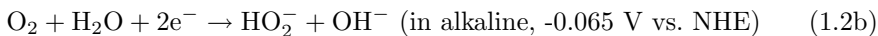
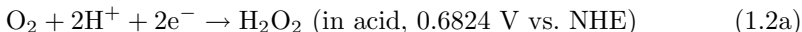


**Fig. 1.1.** Oxygen reduction scheme in acid electrolyte. \*: in the vicinity of catalyst surface, (a): adsorbed on catalyst surface, (b) in bulk solution ([16], copyright Elsevier)

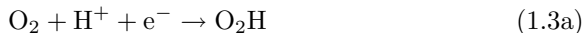
where NHE stands for normal hydrogen electrode as a reference potential. Another and undesirable path is two-electron reduction of  $O_2$ :



for which O–O bond breaking does not occur and peroxide is produced. The most active electrocatalyst for  $O_2$  reduction is found to be Pt and relatives like Pd and Ni, called VIII<sub>a</sub> metals in the periodic table [4]. The goal of electrochemists is to postulate the precise mechanism of ORR on metal catalysts, and then to find a strategy to increase the catalyst activity. Computer simulation results developed in the last decade will be a powerful tool for this purpose.

### Strategy of Electrocatalysts for Oxygen Reduction Reaction

Anderson et al. conducted an ab initio calculation of  $O_2$  reduction [18]. The rate-determining step is assumed to lie on the first electron transfer to  $O_2$  with  $H^+$ ,



followed by several charge transfer steps with  $H^+$ .

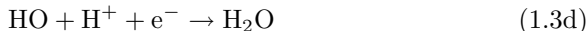
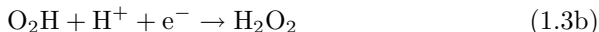
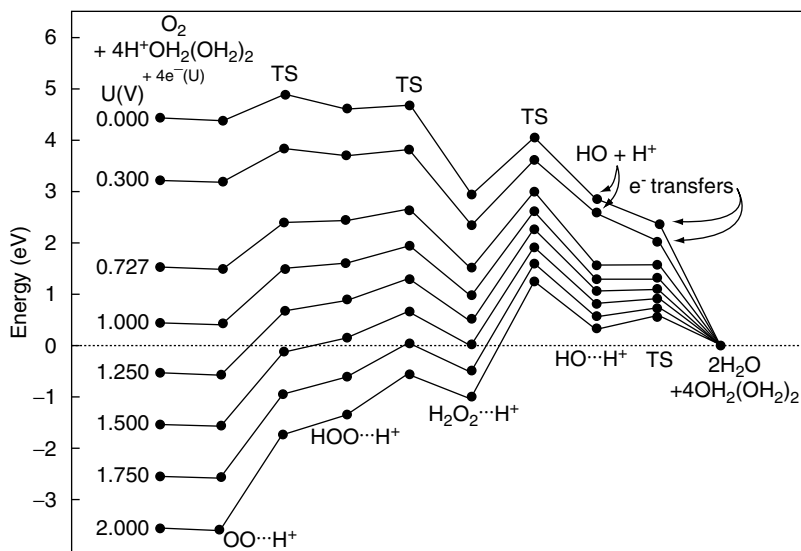


Figure 1.2 shows calculated energies along the reaction sequence (1.3a) to (1.3d). Similar calculations are reported for  $O_2$  attached to Pt atoms, and it is shown that activation energies of the steps (1.3a) and (1.3c) are significantly



**Fig. 1.2.** Energies as functions of electrode potential for the  $\text{O}_2$  reduction sequence. Transition state (TS) and hydrogen bonded precursor ( $\text{O}\cdot\text{H}^+$ ) points are shown [18], copyright the American Chemical Society)

decreased while that of the step (1.3d) is increased [19]. Since the highest barrier of the activation energy resides in the step (1.3c),  $\text{H}_2\text{O}_2$  accumulates during the reaction scheme. The activation of stretching of  $\text{HO}\text{--}\text{OH}$  bond is an important process, for which the catalyst surface needs to provide its reaction field to facilitate the bond breaking. In this respect Zinola et al. reports on interesting results about the adsorption state of  $\text{O}_2$  on  $\text{Pt}(111)$  surface [20]. According to the calculation based on the extended Hückel molecular orbital method, the most stable configuration is bridge side-on contacting two adjacent Pt atoms. Due to the large population of  $\pi^*$  orbitals by  $d$ -electrons from Pt,  $\text{O}\text{--}\text{O}$  bond is weakened [21]. A criteria for a good catalyst for ORR is that the metal supplies sufficient back donation from its  $d$ -band to  $\pi^*$  orbital of  $\text{O}_2$ . This is for the  $\text{O}_2$  in the gas phase, and in the liquid phase the situation will be toward a stable adsorption of  $\text{O}_2$ , but this trend would come to reality especially at negative polarization of the Pt electrode.

Nørskov et al. performed density functional theory (DFT) energy calculation of ORR along the reaction coordinate on various metal catalysts, for both dissociative ( $1/2\text{O}_2 + * \rightarrow \text{O}^*$ , where  $*$  denotes adsorption site on the catalyst surface) and associative ( $\text{O}_2 + * \rightarrow \text{O}_2^*$ ) mechanisms of  $\text{O}_2$  [22]. They defined the maximal activity by using the activation barrier of the rate-limiting step among sequences of elementary steps, and plotted the activity of ORR as a function of the oxygen-binding energy. As shown in Fig. 1.3, a volcano-type curve was obtained and Pt and Pd were found to show a peak activity among transition metals. On the left side of volcano,  $\text{H}^+$  transfer to adsorbed O is

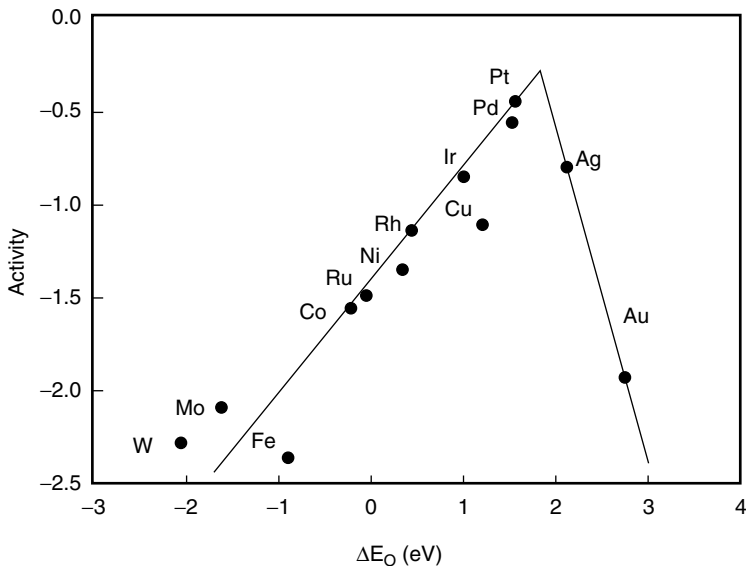
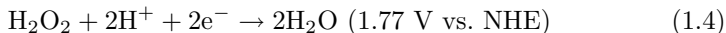


**Fig. 1.3.** Activity of ORR plotted as a function of the oxygen binding energy. ([22], copyright the American Chemical Society)

rate determining, and on the right side,  $H^+$  and  $e^-$  addition to adsorbed  $O_2$  is rate determining. Designing the metal catalyst that shows medium range of M–O binding energy would be preferable for high ORR activity.

Volcano-type curves are also discussed based on d-band vacancies (number of unpaired  $d$  electrons [23]) and % $d$  character of transition metals (the extent of participation of  $d$ -orbitals in the metallic bond [24]), which are related to the adsorbed oxygen intermediate on the metal surface [17]. Figure 1.4 shows log current density plotted against d-band vacancies [25]. Oxygen adsorption that is neither too weak nor too strong looks like a prerequisite for the catalyst surface, which is the pathway of ORR.

In experiments, the mechanism of ORR was discussed with polarization curves in both acid and alkaline media. On dropping mercury electrode, Heyrovsky observed two waves corresponding to (1.2a) for the first step and



for the second step [4]. The following ORR rate–potential relations were verified

$$v = k_c [O_2] \exp \left\{ \frac{-(1-\alpha)FE}{RT} \right\} \quad (\alpha = 0.5, \text{ acid}) \quad (1.5a)$$

$$v = k_c \frac{[O_2][H_2O]}{[OH^-]} \exp \left\{ \frac{-(2-\alpha)FE}{RT} \right\} \quad (\alpha = 0.5, \text{ alkaline}) \quad (1.5b)$$

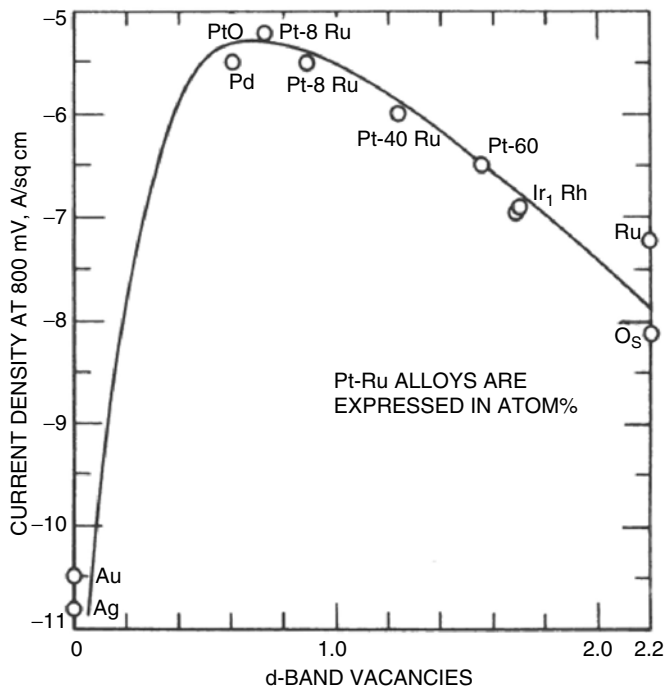


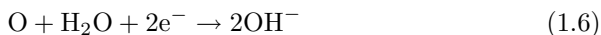
**Fig. 1.4.** ORR current density in 85% orthophosphoric acid at  $-460$  mV RHE at  $25^{\circ}\text{C}$ , plotted against  $d$ -orbital vacancy of the metal ([25], copyright Taylor & Francis)

by Bagotskiy and Yabloova at Hg electrode, and Krasilshchikov at Ag electrode [26]. Bennion derived these rate equations based on the assumption that the first charge transfer (1.3a) is rate-determining in the case of the acid media, and the second step



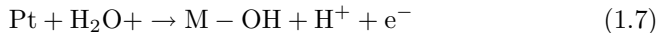
is rate-determining in the case of the alkaline media [27].

Evans proposed the “pseudo-splitting” model of ORR in alkaline media [28]. When  $\text{O}_2$  adsorbs on oxide surface of transition metals, it makes bridge adsorption on the metal or oxide, but not necessarily split into atomic O. Then the surrounding OH groups give the hydrogen to the adsorbed  $\text{O}_2$  like in the Grotthuss hopping, so that in effect bare O atoms are formed at the next site. This bare O site moves to the kink-site on the surface where it gets hydrogen from a water molecule:



If this is the case, the desirable catalyst is to provide active centers for  $\text{O}_2$  (or split O) that gets hydrogen from neighboring water molecules.

In acid solutions, ORR on noble metals is sensitive to the adsorbed oxygen coverage and formation of surface oxides. ORR activity on oxide-free Pt was higher than that on oxidized Pt electrodes [4]. The reaction mechanism on Pt has been argued, based on the observed results: (1) observed Tafel slope was  $2.3RT/F$ , and (2) reaction order at constant potential for  $O_2$  was 1 and for  $H^+$  was  $3/2$  [29]. Assume that Frumkin isotherm holds for reversible Pt-OH formation from  $H_2O$ ,



$$\frac{\theta_{OH}}{1 - \theta_{OH}} = \frac{[H_2O]}{[H^+]} \exp \left\{ \frac{-\Delta G_{OH} - r\theta_{OH} + FE}{RT} \right\} \quad (1.8)$$

which takes into account the repulsive interactions between adsorbed OH [30]. The rate equation for the rate-determining step (1.3a) where vacant site reacts with  $O_2$  and  $H^+$  is written as follows [29].

$$v = k[O_2][H^+](1 - \theta_{OH}) \exp \left\{ \frac{-(1 - \beta)\Delta G_r - \beta(\Delta G_p + r\theta_{OH}) - \beta FE}{RT} \right\} \quad (1.9)$$

where  $\Delta G_r$  and  $\Delta G_p$  are the free energies of adsorption of  $O_2$  and  $O_2H$ , respectively. We get from (1.8) in the medium range of  $\theta_{OH}$  ( $\theta_{OH}/(1 - \theta_{OH}) \approx 1$ ), the Temkin type isotherm:

$$\frac{r\theta_{OH}}{RT} = -\ln H^+ + \frac{FE}{RT} - \frac{\Delta G_{OH}}{RT} \quad (1.10)$$

Substitution of (1.10) into (1.9) yields

$$v = k[O_2][H^+]^{1+\beta} \exp \left\{ \frac{-(1 - \beta)\Delta G_r + \beta(\Delta G_{OH} - \Delta G_p) - 2\beta FE}{RT} \right\} \quad (1.11)$$

which for  $\beta = 0.5$  accords with the experimental results (1) and (2). This result means that the presence of OH on Pt more or less hinders the start of ORR. When  $\theta_{OH} \rightarrow 0$ , (1.9) gives the Tafel slope  $2.3 \times 2RT/F$ , which is also observed at large overpotential range. Whether  $O_2$  reduction proceeds via direct four-electron path or via two-stage path with  $H_2O_2$  as an intermediate is a matter of debate among electrochemists. Although  $H_2O$  yield of ORR is more than 98% on Pt,  $H_2O_2$  production is shown to occur in the case of anion specific adsorption or of atomic H adsorption at  $<0.3$  V vs. NHE.

Watanabe et al. give a strategy for designing Pt alloy catalysts that provide high ORR activity on the basis of d-band modification by the second element [31]. Figure 1.5 illustrates the  $O_2$  bonding mode and the change of electronic structure of Pt induced by the second element. The best composition of the alloy corresponds to the condition where high probabilities of both the donation from  $\pi$  orbital of  $O_2$  to  $d_{z^2}$  orbital of M and the back donation from partially filled  $d_{xz}$  and  $d_{yz}$  orbital of M to antibonding  $\pi^*$  orbital of  $O_2$

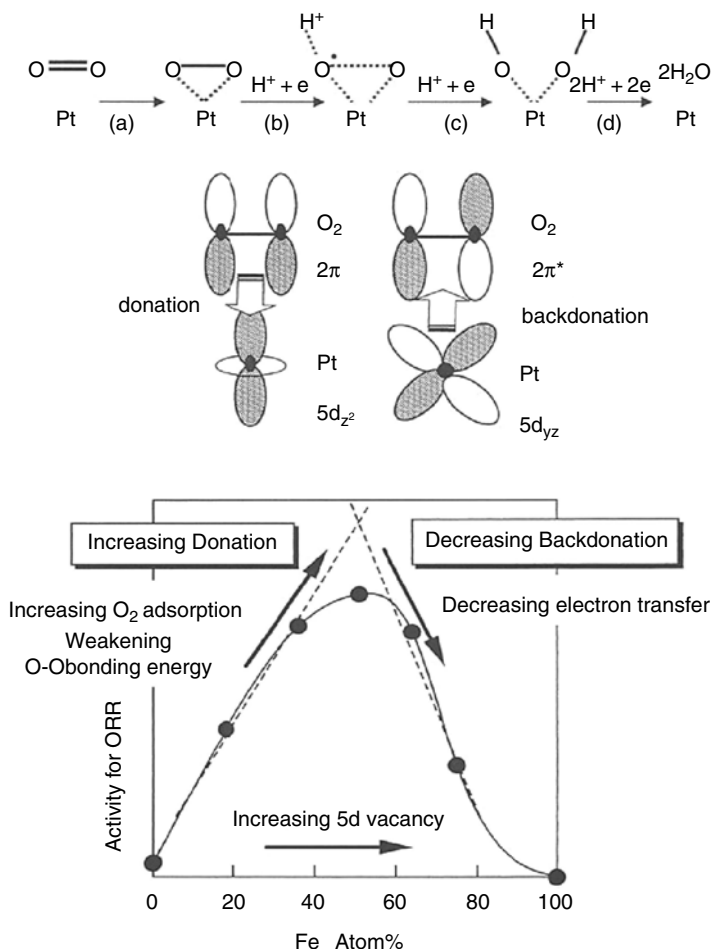


**Fig. 1.5.** Proposed mechanism of the enhancement of ORR by alloying Pt with Fe-group metals ([31], copyright The Electrochemical Society)

are satisfied. In addition to the electronic structure of the metal, the importance of the geometric factor such as the interatomic distance of metals was pointed out by Jalan et al. [32]. In ORR involving lateral adsorption of  $\text{O}_2$  on the catalyst surface, the interatomic distance would affect the adsorption and O–O bond rupture, and then the catalytic activity.

In conclusion, best ORR catalysts will be achieved by aiming at materials that have (1) medium range of M–O bonding energy, (2) large population of  $\pi^*$  orbital of  $\text{O}_2$  by  $d$ -electron back donation from M so that O–O bond weakens, (3) smallest oxide formation even at potentials 1.0 V NHE, (4) high rate of  $\text{H}^+$  addition from neighboring  $\text{H}_2\text{O}$  on the catalyst surface, and (5) anticorrosive nature in acid media. Bockris et al. mentioned as indirect methods the use



of redox mediators to change the path of ORR, for example  $\text{HNO}_3/\text{NO}$  that shows faster reduction and oxidation rates than  $\text{O}_2$  [4].

### Oxygen Reduction Reaction on Macrocycles

The spin structure of  $\text{O}_2$  (triplet) restricts the reactivity of  $\text{O}_2$  with molecules having singlet ground states, but this spin restriction is overcome when  $\text{O}_2$  coordinates to metal centers of macrocycles [10]. In ORR,  $\text{O}_2$  interacts and receives electrons from the metal center. In the course of the reaction, two intermediate states should be experienced, (1) the metal center is reduced to lower valence state, (2) oxygen molecule adsorbs on the central metal ion to interact electronically with the macrocyclic molecule. (3) Further to make sure the four-electron reduction of  $\text{O}_2$  to  $\text{H}_2\text{O}$ , cleavage of O–O bond should occur through the reaction scheme.

Typical examples of metal macrocycles are metalloporphyrins and metalphthalocyanines (Fig. 1.6). The use of macrocycles to ORR catalysts was first reported by Jasinski in mid-1960s [9], and was applied as a fuel cell cathode [33]. These macrocyclic complexes can bind a dioxygen molecule to the metal center in the N4 moiety, and transfer electrons via conjugated aromatic rings surrounding the active center. Prior to this electron transfer, the central metal ion should be reduced from M(III) to M(II) state. Randin proposed the concept of redox catalysis where the redox potential of the central metal plays an important role [34]. According to Lever et al. the central metals should have accessible  $d$ -orbitals located at the level between highest occupied molecular orbital (HOMO) and lowest unoccupied molecular orbital (LUMO) of the macrocycles [10]. Metals that meet the above two conditions are mostly transition metals with partially filled  $d$ -electron orbitals (group VI<sub>a</sub> to VIII).

The role of a macrocyclic molecule surrounding the metal center can be considered in two ways:

1. Macrocycles modify the electronic structure of metal and relocate its redox potential so that  $\text{O}_2$  can accept electrons from half-filled metal  $d$ -orbitals.
2. Macrocycles are mediators that connect the electronic levels of  $\text{O}_2$  and the metal if those are too far apart, and ease the transition of electrons.

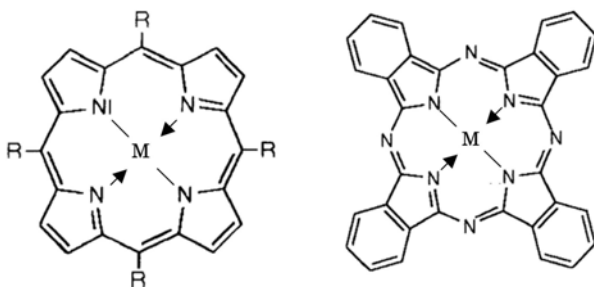


**Fig. 1.6.** Porphyrin and phthalocyanine complex structures. M = transition metal

As regards the former mechanism, macrocycles shift the redox potential of the metal to negative directions, and drive from M(III) to M(II) state. This would facilitate the electron transfer from M to O<sub>2</sub> [34]. Concerning the latter mechanism, Hoffmann et al. suggested that the energy of the  $\pi^*$  HOMO of O<sub>2</sub> should lie close to the level of d-band energy of M, in order to form the most favorable intermediates that bind the ligand O<sub>2</sub> with extra-planar configuration [35].

About the catalytic activity of a metal chelate in relation to its redox potential, two kinds of correlations are reported. In the case (1) stated above, the linear correlations are expected as discussed by Randin [34] and Zagal et al [36]. In the case (2), the volcano shaped curve would be expected because the energy of *d*-orbitals in macrocycles decreases linearly on going from Mn to Ni on the periodic table as calculated by Taube [37], where the energy level of O<sub>2</sub> HOMO should lie. Linear and volcano-type plots examined experimentally are illustrated in Fig. 1.7 [36] and Fig. 1.8 [38]. There are other factors such as the change of rate-determining steps or the difference of mechanisms of four-electron or two-electron O<sub>2</sub> reduction. In Fig. 1.7, Fe or Mn phthalocyanines reveal M(III)/M(II) redox potentials that are close to the potential of ORR and promote four-electron mechanism, while on Co phthalocyanines ORR takes place at a potential very far from that of M(III)/M(II) couple and proceeds with two-electron mechanism. Therefore the explanation of the ORR activity and the redox potential relations needs careful study.

Two types of interactions can be assumed for the central *metal*-dioxygen complex. One is the side-on structure (Griffiths model) and the other is the end-on structure (Pauling model), the former may be further categorized into

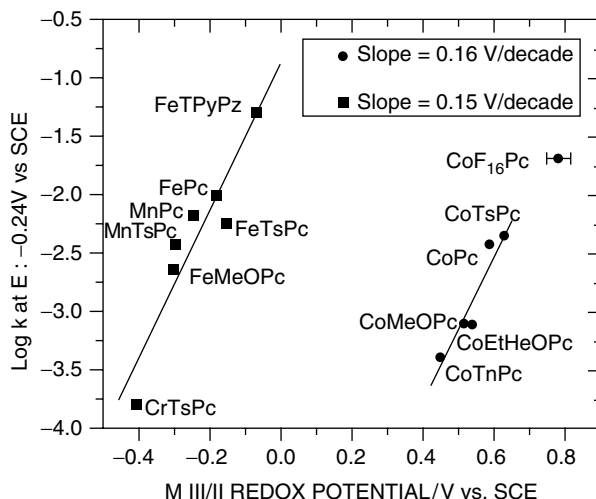


**Fig. 1.7.** ORR activity of various metallophthalocyanines in 0.1 M NaOH plotted against the first oxidation potential ([36], copyright Pergamon Press)

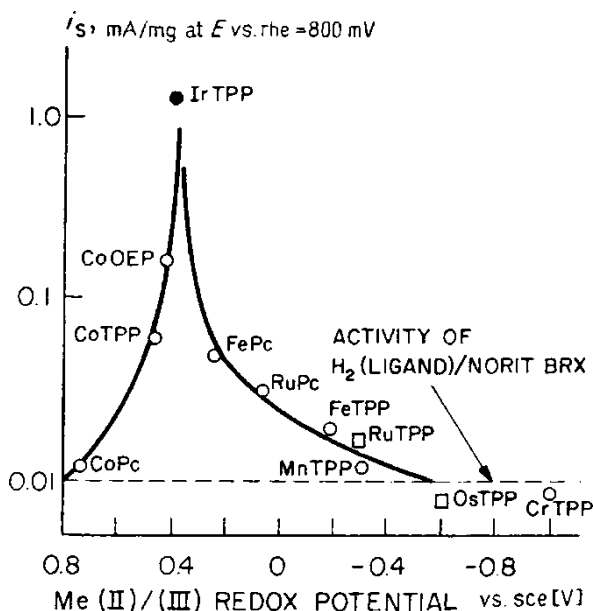


**Fig. 1.8.** ORR activity of various metallophthalocyanines in 4M  $\text{H}_2\text{SO}_4$  plotted against the redox potential ([38], copyright Verlag Chemie GmbH)

1:1 and 2:1 coordination according to the number of sites per  $\text{O}_2$  molecule (Fig. 1.9 [39]). Upon coordination of the  $\text{O}_2$  molecule to a metal center,  $2p$  electrons of  $\text{O}_2$  interact with  $d$ -orbitals of the metal through (1) a  $\sigma$ -type bond by donation from bonding orbital of  $\text{O}_2$  to acceptor orbital  $d_{z^2}$  of the metal and (2) a  $\pi$ -backbond interaction between the  $d\pi$  ( $d_{xy}, d_{yz}$ ) orbital of the metal and the partially occupied  $\pi^*$  antibonding orbital of  $\text{O}_2$ .

Collman et al. synthesized dicobalt cofacial porphyrin dimers in which two porphyrin rings were constrained in parallel by two amide bridges of varying length, and found that four-atom bridges produced good four-electron reduction of  $\text{O}_2$  [40]. Yeager discussed the four-electron reduction efficiency and the coordination of  $\text{O}_2$  on metal complexes [39,41], based on the data of Collman et al. and of Liu et al. [42]. A *cis*-configuration of  $\text{O}_2$  between two metal centers separated by about 0.4 nm was the most efficient structure for  $\text{O}_2$  reduction. The assumed mechanism was that a *cis*- $\mu$ -peroxo intermediate formed between  $\text{Co(II)}\text{-Co(II)}$  of two porphyrin rings favors  $\text{H}^+$  access and  $\text{O-O}$  bond rupture. However, Mn and Fe phthalocyanine monomers also showed direct reduction of  $\text{O}_2$  to  $\text{H}_2\text{O}$  [31]. This was attributed to the catalytic ability of phthalocyanines for chemically decomposing  $\text{H}_2\text{O}_2$  to  $\text{H}_2\text{O}$ . The second reasoning was the mode of interaction of  $\text{O}_2$  with the metal centers. For iron phthalocyanines, side-on configuration was preferred and  $\text{O-O}$  bond cleaving was promoted by back donation of  $d$ -electrons from the metal center. Fast exchange of  $\text{M(III)/M(II)}$  couple was also a prerequisite for four-electron reduction of  $\text{O}_2$ .

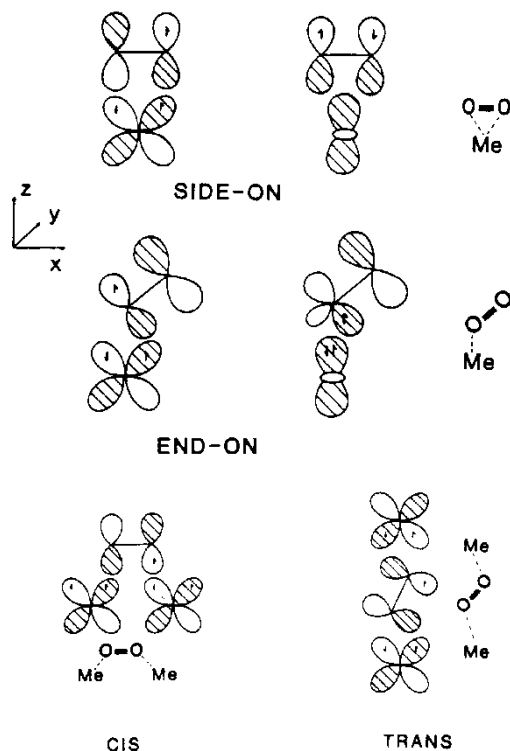


**Fig. 1.9.** Various types of interactions of  $O_2$  with transition metal species ([39], copyright Elsevier)

### 1.2.2 Fuel Oxidation Catalysts

As fuels hydrocarbon (methanol, formic acid, ethanol, dimethylether, etc.) can be the candidate besides  $H_2$ , but environmental and hazardous concerns to humans in addition to energetic considerations limit the fuels to only a few [43]. In this section  $H_2$ , methanol, and formic acid oxidation, and the topic of CO poisoning will be discussed especially with future possibility of macrocyclic or metal complex catalysts.

### Hydrogen Oxidation Catalysts and CO Poisoning

Reaction of  $H_2$  on metal electrodes has been the most frequently studied subject among electrochemists. The cathodic reduction of  $H^+$  to  $H_2$ , the hydrogen evolution reaction (HER) has many basic and common features to other electrochemical systems, and many reviews and publications have been historically done so far [44–46]. Important results were obtained in 1957 when Conway and Bockris found a linear relationship between the exchange current density  $\log i_0$  of HER and the work function of metal electrodes [47]. A volcano

curve correlation between  $\log i_0$  and the heat of adsorption of H on metals was reported in 1958 by Parsons and Gerischer, based on the transition state theory [46]. Kita et al. reported a periodic change of  $\log i_0$  when plotted against the atomic number of metals, with a peak around Pt [6]. They investigated the correlations between  $\log i_0$  and various physical parameters of metals, and concluded that the most important factors to be the work function and heat of adsorption of hydrogen. They categorized metals into “d-metals” (transition and Ib metals in the periodic table) and “sp-metals” (metals after IIb) for which the HER reaction intermediates are the adsorbed hydrogen atom H(a) and the adsorbed hydrogen molecule ion  $\text{H}_2^+$  (a), respectively.

Comparing to HER, the anodic reaction of  $\text{H}_2$  to  $\text{H}^+$  (hydrogen oxidation reaction, HOR), although acknowledged as the important reaction in fuel cells, gathered rather smaller number of reviews until the last decade. This is due to the experimental restrictions for  $\text{H}_2$  reactions, where gaseous reactants should be supplied under controlled manner rather than the reactants in the electrolyte. In 1990s the number of literatures surged especially in the design of CO-tolerant metal or alloy catalysts for fuel cell applications. The HOR mechanism in acid media is based on the slow Tafel step followed by fast Volmer step [46]:



At least two types of  $\text{H}_{\text{ad}}$  are acknowledged, on-top H and hollow-site UPD H on the Pt crystal surfaces.

Most of the literatures discuss the CO or anion adsorption to characterize the HOR on Pt electrodes. The tailor-made surface approach of the catalyst is the recent trend of researches, which looks for the good design of CO-tolerant anode catalysts after studying the facets of single crystals or sub-monolayer of second elements. Techniques developed before 1990s, for example, scanning tunneling microscope (STM), atomic force microscopy (AFM), and in situ spectroelectrochemical methods greatly assisted in observing structural sensitivity of the reacting catalyst surfaces under polarization measurements. According to the recent results, kinetics of HOR and of CO oxidation on Pt is strongly influenced by the crystal facets, anion adsorption, and oxidation of Pt surfaces [46]. In sulfuric acid solutions, Pt(111) surface shows the least reactive and the highest activation energy among single crystal surfaces, considering its high surface atomic density ( $1.53 \times 10^{15}$  atoms  $\text{cm}^{-2}$ ) that results in the high energy of interaction with anions.

The first nonprecious metal catalysts for HOR were tungsten carbide (WC),  $\text{WS}_2$ , and  $\text{MoS}_2$  [48]. The remarkable point was no CO poisoning, but the fuel cell performance was not satisfactory. HOR catalysts based on organic metal complexes are so far rather few. Crystal structure of heterodimeric hydrogenase enzymes is recently published [49], and its model with a nickel–ruthenium dinuclear aqua complex forming a bridging hydrido ligand,

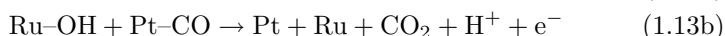
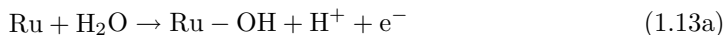
Ni( $\mu$ -H)Ru is reported to oxidize H<sub>2</sub> into H<sup>+</sup> in aqueous solutions at 20°C [50]. Based on biomimetic approach using DFT calculations of nitrogenase active sites, Nørskov et al. proposed MoS<sub>2</sub> as potential electrocatalyst for HER [51]. Further developments in search for practical HOR catalysts are expected in the near future.

## Hydrocarbon Oxidation Catalysts

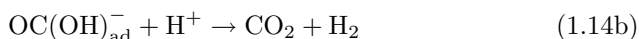
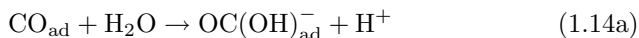
Direct methanol fuel cell (DMFC) is acknowledged as a “dream fuel cell” among electrochemists because this fuel cell enables a simplified system without the need for fuel reformers and other parasitic systems, a high power density that exceeds lithium ion batteries and easy storage or recharging of fuels [52]. Especially as power sources for small-scale devices such as mobile phones, laptops, and personal digital assistance (PDA), DMFC has many advantages over existing energy sources, and the projected performance can easily satisfy the future cost target. In the last decade, study of DMFCs increased both for the system and for component materials [53]. Since one of the major problems with DMFC is low activity of methanol oxidation reaction, the catalyst research attracts many electrochemists as ever-increasing topics [54, 55].

For methanol oxidation, Pt–Ru alloy has been the most studied catalyst for more than 40 years, but alternatives have been pursued in many possibilities. Those examples were platinum based alloys (Pt–Sn, Pt–Mo, Pt–Ni, Pt–Fe) [56, 57], platinum finely dispersed on oxide supports like TiO<sub>2</sub>, MoO<sub>2</sub>, WO<sub>3</sub>, etc [58–62]. New base catalysts were proposed, e.g., mixture of nickel-tungsten alloy and WC prepared from nickel tungstate [63]. New types of catalysts were also proposed, e.g., rare earth cuprates [64], or organic metal complexes as a cocatalyst with platinum [13, 65–68]. In the study of the electrochemical CO oxidation on carbon-supported and heat-treated metal porphyrins, van Baar et al. found Rh, Ir, and Co chelates as good electrocatalysts, and proposed a mechanism similar to the water gas shift reaction [69]. Bett et al. reported the enhancement of methanol oxidation on Pt cocatalyzed with Sn and Ru macrocycles, and discussed the activity in relation to their redox potentials [13].

As the mechanism of methanol oxidation on Pt, dual paths, i.e., CO path, and non-CO path are considered as possible routes [70]. Non-CO path (direct path) assumes formate species (HCOO<sub>ad</sub>) as an intermediate, and this changes into CO<sub>2</sub> as a reaction product [71]. CO path (indirect path) makes a poison that strongly adsorbs on the catalyst surface. To cope with this problem, several concepts for CO-tolerant catalysts for methanol oxidation are proposed so far. For example, as possible mechanisms in Pt–Ru alloy, two points are noticed to consider a role of Ru element. One is the bifunctional mechanism, and Ru provides a site of oxygen-containing species, and oxidizes CO that adsorbs on Pt site [72, 73].



Due to the presence of OH on Ru derived from H<sub>2</sub>O, CO can be oxidized at a lower potential (0.4 V vs. NHE) than on pure Pt (0.6 V vs. NHE). The second idea is called the ligand mechanism, in which Ru weakens CO bonding on Pt by inducing *d*-electron deficiency in the electronic structure of Pt, thus catalyzing the oxidation of CO at potentials much lower than that observed for Pt [74]. Whether or not these mechanisms also apply for the catalysis involving macrocycles is still a matter of debate, but it is interesting to refer to the basic idea of van Baar et al. who worked on metal macrocycles for CO oxidation and ascribed the mechanism similar to that of the water gas shift reaction [69].



On metal macrocycles CO<sub>ad</sub> is polarized as  $-\text{C}^{\delta+}=\text{O}^{\delta-}$ , and this induces a nucleophilic attack of H<sub>2</sub>O from the surrounding, resulting in hydroxycarbonyl species  $-\text{CO}(\text{OH})^-$ , from which H is pulled off and CO<sub>2</sub> emerges. A support for this mechanism is that CO can be oxidized to CO<sub>2</sub> even in a full coverage of CO, because H<sub>2</sub>O can be supplied from the surroundings (Rideal–Eley mechanism). This is in contrast to the case of bifunctional mechanism, where a site for OH<sub>ad</sub> is required to oxidize CO<sub>ad</sub>, both of which are adsorbed species coming from the atmosphere (Langmuir–Hinshelwood mechanism).

Formic acid oxidation is acquiring attention in recent years because of the increasing needs of developing small-scale fuel cells for portable devices [75]. Although formic acid has lower specific energy of 1,630 Wh kg<sup>-1</sup>, as compared with methanol (6,073 Wh kg<sup>-1</sup>), the former has the advantage that theoretical cell voltage 1.40 V exceeds that of methanol (1.21 V) and the fuel crossover through the polymer electrolyte is low, which is a major problem for methanol [43]. This is because anionic species dissociated from formic acid is rejected from entering in the polymer electrolyte membranes. As in the case of DMFC, formic acid oxidation shows large overpotential, and the fuel catalyst is a crucial topic for the commercialization of fuel cell [76].

The best catalyst studied so far are Pt–Pd alloy and Pd nanoparticles [75, 77]. Recent research proposes new materials such as Pt with submonolayer-deposited Pb (PtPb<sub>UPD</sub>) [78], Bi-modified Pt [79], intermetallic phases of Pt–Bi, Pt–In and Pt–Pb [80]. Use of macrocyclic compound tetrasulfophthalocyanine as a cocatalyst for Pt is a new challenge as a formic acid oxidation promoter [15]. Although the mechanism of formic acid oxidation is not yet clarified as that of methanol, CO and formate are observed on Pt surface, and similar mechanisms are considered as for methanol oxidation reaction that involve the active intermediate and the poisoning intermediate [81–84].

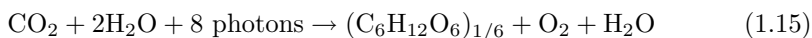
Bemirci, based on the theoretical work by Nørskov et al. [85], interpreted the behaviors of alloy catalysts [86]. Two concepts are introduced:

1. One is the shift of d-band centers of surface atoms by overlayers calculated by DFT, which through the chemisorption energy of reacting molecules determines the reactivity of the alloy.
2. The second is the segregation energy that determines the configuration of alloy elements on the catalyst surface.

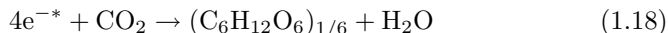
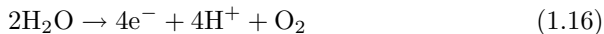
The geometric effect is ignored. According to the criteria, good alloys like Pt–Ru can be selected by seeking the negative shift (weak adsorption) of d-band centers for metals suffering from poisoning by CO-like species (Pt), and positive shift (strong adsorption) for elements that provide OH species (Ru). Also segregation affects the surface atomic composition, and the metal that provides multiple sites for the reactant should segregate while the other element offering OH should anti-segregate. On the other hand, for HCOOH oxidation, the second element should reduce the number of CO adsorption sites on Pt by geometric hindrance (third-body effect). Thus Pt should anti-segregate and d-band center shifts up while those of the second element remains constant, which applies well for Pt–Au and Pt–Pd alloys.

### 1.3 Molecular Catalysts for Artificial Photosynthetic Reaction

Photosynthesis is the most important energy conversion system on our earth. It supports almost all the biological energies by converting solar energy into chemical energy by utilizing an extremely sophisticated and complicated molecule based system. The photosynthetic system will be shown in Chap. 8; the important point of photosynthesis is represented by the (1.15) where carbon dioxide and water is reacted by utilizing solar visible light photons to produce a main product, carbohydrate, shown by  $C_6H_{12}O_6$ .



This reaction is represented by the following three major processes (1.16), (1.17), and (1.18), where water is an electron donor providing electrons to the whole system (see also Chap. 8). The electrons obtained from water at the Mn protein complex (1.16) are excited by solar photons at the chlorophyll reaction center (two steps) to form high energy electron ( $e^{-*}$ ) (1.17), and the  $e^{-*}$  reduces  $CO_2$  to carbohydrate (1.18) via reduction of NADP to NADPH.



This process is represented by Fig. 8.1 shown later where the electron from water is driven by two steps (at the Photosystems II and I, abbreviated to PSII and I) at the reaction center chlorophyll to higher energy, and finally reduces



CO<sub>2</sub> to produce carbohydrate. Molecular metal complexes and metal clusters play an important role in photoinduced electron transfer and catalysis.

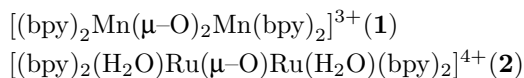
In Sects. 1.3.1, 1.3.2, and 1.3.3, the important water oxidation catalysts, reduction catalysts, and photoinduced chemical reactions for devices will be described.

### 1.3.1 Water Oxidation Catalyst

Catalytic water oxidation (dark reaction) is the first and important reaction of the electron flow in the photosynthesis represented by Fig. 8.1 (see Chap. 8) where water is used as a source of electrons provided to the whole system. Since water oxidation is so important for the biological activities, its catalyst and reaction mechanism have been reported in many books and reviews [87–93].

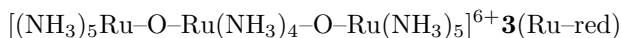
In the photosynthesis a Mn-protein complex works as a catalyst for the difficult four-electron oxidation of two molecules of water to form one O<sub>2</sub> molecule (1.16). It is inferred that at least four Mn ions are involved in the active center, but its structure is not yet completely elucidated.

Molecular metal-containing catalysts for water oxidation have been attracting attention a great deal as models for the photosynthetic catalyst. Many structural models have been synthesized [93]. Among them, tetrakis(2, 2'-bipyridine)(di-μ-oxo)di-Mn complex (**1**) and tetrakis(2, 2'-bipyridine)(μ-oxo) di-Ru complex (**2**, Meyer's complex) are typical examples that showed some activity for water oxidation, but the activity was not high enough for water oxidation.



Water oxidation catalysis has been studied both by chemical method (Fig. 1.10a) using Ce(IV) as oxidant and electrocatalytic method (Fig. 1.10b) using polymer-coated electrode [91–93].

It has been found that ammine-ligand-based Ru complexes, trinuclear, dinuclear, and mononuclear ones, show high activity as catalysts for water oxidation [91–93]. Because the catalyst – trinuclear Ru–ammine complex called Ru–red (**3**) – is very active, it can even evolve observable O<sub>2</sub> bubbles in the presence of a strong oxidant such as Ce(IV) ion in water.



### 1.3.2 Reduction Catalyst

When aiming to establish a real photosynthesis model, the CO<sub>2</sub> reduction must be considered as the reaction part for the gain of fuels. As shown in previous literature [94], in a thermodynamic sense, the multi-electron reductions of CO<sub>2</sub> particularly into CH<sub>4</sub> as well as CH<sub>3</sub>OH are more favored than

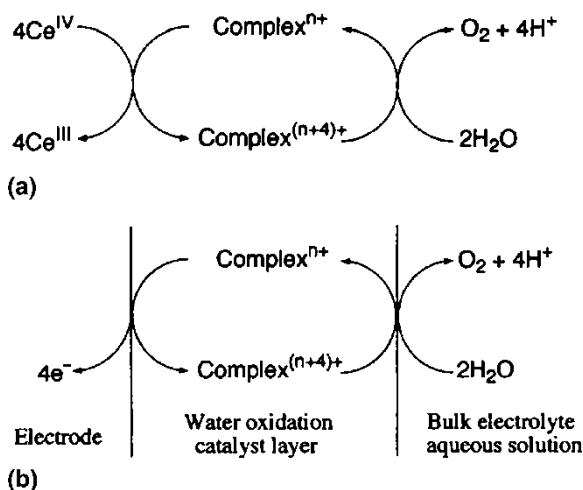


**Fig. 1.10.** Chemical water oxidation catalyst represented by  $\text{Complex}^{\text{n}+}$  (a) and electrochemical water oxidation catalyst (b)

the  $\text{H}^+$  reduction into  $\text{H}_2$ . However,  $\text{CO}_2$  activation is essentially difficult due to its stable structure (considering the bond moment of  $\text{C}-\text{O}(\text{CO}_2, 2.3\text{D})$  [95], C is positively charged, while O is negatively charged;  $\text{CO}_2$  is expected to act as an electron acceptor rather than an electron donor due to its high ionization potential [96], which means that the C atom in  $\text{CO}_2$  is the activation point). Therefore, all  $\text{CO}_2$  reductions have poor feasibility in a kinetic sense, suggesting that a highly efficient and active catalyst site must be fabricated via catalysis chemistry. The potential for various kinds of metal complex to act as catalysts for  $\text{CO}_2$  reduction has been studied via photochemistry and electrochemistry; however, there has been no example of a photoinduced  $\text{CO}_2$  reduction along with the electron donation originating from water oxidation, although the chemical activation of  $\text{CO}_2$  is now the focus of continuous attention.

It is possible to replace  $\text{CO}_2$  fixation by the  $\text{H}^+$  reduction into  $\text{H}_2$  in order to establish a water photolysis system. It has been known that Pt and its colloidal particles are the most active catalysts for the reductions of  $\text{H}^+$  as well as  $\text{O}_2$  [17, 97–99]; however, Pt is a rare and precious material. According to statistical data [100],  $\sim 1.0 \times 10^5$  kg of Pt corresponding to 45% of overall demands (in 2003) is used as catalyst, making it highly desirable to design and develop a new catalyst alternative to Pt, especially using molecular catalysts.

In the present section, typical examples of molecule-based catalysts for  $\text{CO}_2$  and  $\text{H}^+$  reductions will be shown.

## CO<sub>2</sub> Reduction Catalyst

### *Metallophthalocyanines*

The catalyses of metallophthalocyanine (denoted as MPc for the 1:1 complex) and its derivatives for CO<sub>2</sub> reduction have been extensively studied [e.g., 101, 102]. It has also been acknowledged that a metal-free phthalocyanine is incapable of CO<sub>2</sub> reduction [103], suggesting that interaction between a metal ion and CO<sub>2</sub> is essential for the catalytic reduction; in addition, a metallodiphthalocyanine with a sandwich-structure (i.e., the 1:2 complex of MPc<sub>2</sub>) was also applied to the CO<sub>2</sub> reduction [104], but the MPc<sub>2</sub> exhibited poor catalysis due to little opportunity for the CO<sub>2</sub> coordination to metal ion.

Among the MPcs of monophthalocyanine, CoPc is the most typical and active electrocatalyst, which often results in CO formation [101, 102, 105–109]; however, in the water phase, the H<sup>+</sup> reduction into H<sub>2</sub> takes place competitively (selectivity (CO/H<sub>2</sub> ratio), ~1.5 : 1 [105]). Therefore, the development of a much more kinetically efficient catalyst site in CO<sub>2</sub> reduction process than in H<sup>+</sup> reduction has been the focus of attention in order to accomplish selective CO<sub>2</sub> reduction in an aqueous media as well as fabricate a real reduction site towards an artificial photosynthetic model. The use of a polymer matrix as a catalyst supporter was effective for an active and selective CO<sub>2</sub> reduction [106, 107]. The catalyst membrane composed of CoPc and poly(4-vinylpyridine) (PVP) performed active and selective CO<sub>2</sub> reduction in comparison with a neat CoPc coating (selectivity (CO/H<sub>2</sub> ratio), ~4 : 1) [107]. This was ascribed to the coordinative and weakly basic properties of PVP; namely, the coordination of PVP to CoPc can cause an increase in electron density on the Co ion, which facilitates the intermediate formation; furthermore, the weakly basic property of PVP can favorably function as a H<sup>+</sup> source for the dehydration process in producing CO from CO<sub>2</sub>.

The CoPc derivatives substituted with the butoxy group (CoPc(BuO)<sub>8</sub>) [108] or the cyano group (CoPc(CN)<sub>8</sub>) [109] can also exhibit active catalysis for CO<sub>2</sub> reduction (*cf.* activity: CoPc(BuO)<sub>8</sub> > CoPc > CoPc(CN)<sub>8</sub>). Those show typical characteristics for redox catalysis affected by the electronic property of the complex employed. When substituting CoPc for the electron-donating group, the electron density of the CoPc(BuO)<sub>8</sub> becomes high in comparison with the others, affecting the redox potential in the form of CoPc(BuO)<sub>8</sub> (negative) < CoPc < CoPc(CN)<sub>8</sub> (positive). Therefore, in a highly basic CoPc(BuO)<sub>8</sub> system, an electrophilic addition reaction of CO<sub>2</sub> onto CoPc(BuO)<sub>8</sub> (CO<sub>2</sub>-adduct formation) is expected to take place favorably, which efficiently induces reduction catalysis.

The electronic property of the CoPcs can also be the key factor affecting their catalysis mechanisms. Catalysis by CoPc for CO<sub>2</sub> reduction has been considered to take place through the two-electron reduced species. However, it appeared that the electrocatalytic CO<sub>2</sub> reduction by CoPc takes place at a more negative potential than the second reduction of Co(II)Pc, which may

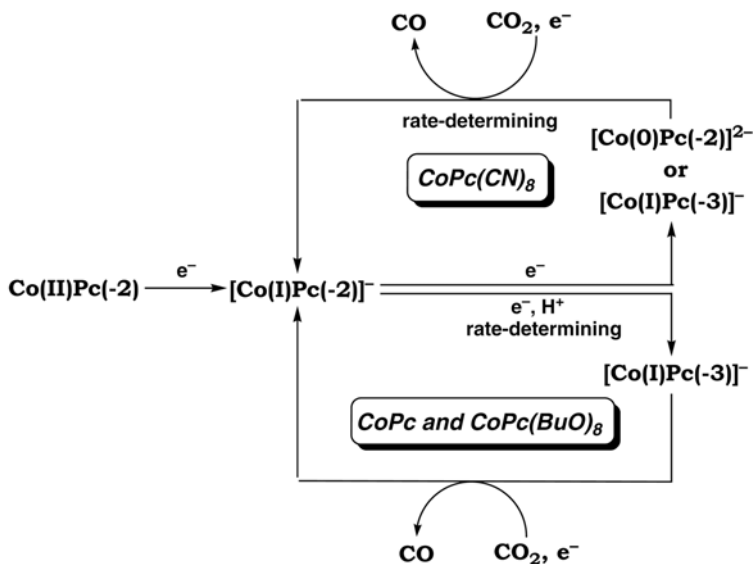


**Fig. 1.11.** Proposed mechanisms of electrocatalytic CO<sub>2</sub> reduction by the CoPc and its derivatives ([109], copyright Wiley)

indicate the involvement of a further reduced species of CoPc with the CO<sub>2</sub> reduction. In order to elucidate the catalysis mechanism, an in situ potential-step chronoamperospectroscopy (PSCAS) was conducted in a pyridine solution containing the CoPcs. Based on the PSCAS results, the mechanisms of CO<sub>2</sub> reduction by the CoPcs were proposed (Fig. 1.11) [107–109].

### *Polypyridyl Metal Complexes*

Tanaka et al. have studied and clarified the catalysis of polypyridyl ruthenium complexes involving carbonyl ligand in organic solution (Fig. 1.12) [110–113]. In those catalyses, the complex (e.g.,  $[\text{Ru}(\text{bpy})_2(\text{CO})_2]^{2+}$  (bpy = 2,2'-bipyridine)) usually underwent reductive cleavage of the Ru–CO bond to form CO under electrochemical conditions, whereupon the reduced species ( $[\text{Ru}(\text{bpy})_2(\text{CO})]^0$ ) reacted with CO<sub>2</sub> to recover the original complex. When employing the specific conditions (such as a low temperature [111], an introduction of a ligand (such as naphthylpyridine) leading to a stabilization of the Ru–CO in complex [112, 113], etc.), the reductive cleavage of the Ru–CO can be suppressed, resulting in higher reduction products such as HCHO [111], CH<sub>3</sub>OH [111], and CH<sub>3</sub>COCH<sub>3</sub> (in the presence of the alkylation reagent (CH<sub>3</sub>I)) [113].

A number of molecule-based catalysts, including MPc, are water-insoluble, and those catalyses in the water phase have usually been investigated within a heterogeneous system. For example, the preparation

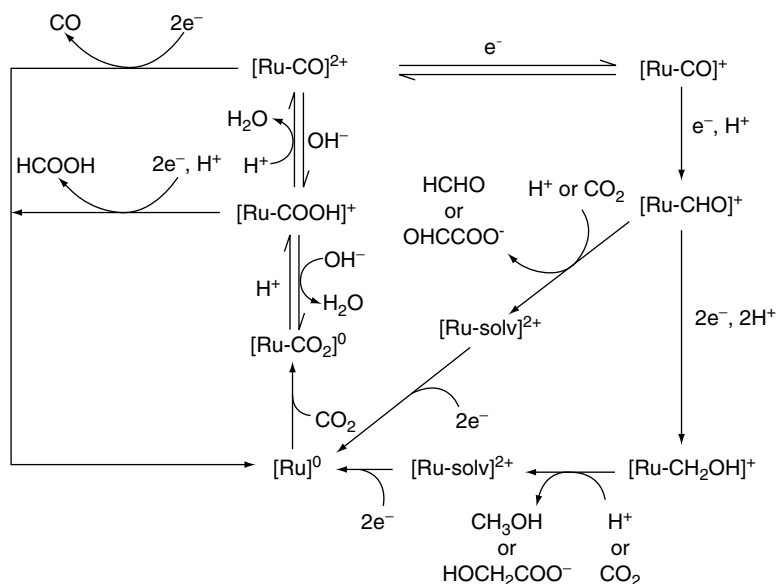


**Fig. 1.12.** Formation pathways of HC(O)H, CH<sub>3</sub>OH, H(O)CCOOH, and HOCH<sub>2</sub>COOH by polypyridyl ruthenium complexes involving carbonyl ligands ([111], copyright the American Chemical Society)

of a modified electrode was particularly effective in elucidating the molecular catalysis of the water-insoluble complex in the water phase. By embedding such a complex into a water-insoluble polymer and confining it to an electrode surface, the heterogeneous catalyst system of a molecular aggregate can be formed, which may also show unique and/or active catalysis that cannot be achieved using a homogeneous solution or a neat catalyst [114]. Employing a polypyridyl noble metal complex of carbonyl ligand (e.g.,  $[Ru(bpy)_2(CO)_2]^{2+}$  [115],  $[Ru(L)(CO)_2(CH_3CN)]_2^{2+}$  (L = pyrrole-substituted bpy) [116],  $[Re(bpy)(CO)_3Cl]^{2+}$  [117], etc.) as a catalyst in a polymer matrix, metal-metal bonding occurred due to the molecular aggregation of the complex, which leads to an efficient and selective CO<sub>2</sub> reduction in the water phase.

Polypyridyl-type transition metal complexes have also been studied for their potential catalytic activity for CO<sub>2</sub> reduction [118–121].  $[Co(terpy)_2]^{2+}$  (terpy = 2, 2' : 6', 2''-terpyridine) embedded in a Nafion membrane exhibited catalysis for a selective formate formation (selectivity (HCOOH/H<sub>2</sub> ratio), ~4 : 1) [118], for which bimolecular catalysis by  $[Co(terpy)_2]^+$  (one-electron reduced species) is proposed. Such a cooperative catalysis is also a typical characteristic of molecular aggregates of which catalyst molecules are closely arranged within a polymer matrix. 4-Vinylterpyridine (4-v-tpy) complexes of Cr, Ni, Co, Fe, Ru, and Os have been prepared and assessed for CO<sub>2</sub> reduction